3 1176 00503 6471

RESEARCH MEMORANDUM

A COMPARISON OF THREE THEORETICAL METHODS OF CALCULATING SPAN LOAD DISTRIBUTION ON SWEPT WINGS

By

Nicholas H. Van Dorn and John DeYoung

Ames Aeronautical Laboratory
Moffett Field, Calif.

CLASSIFIED DOCUMENT

This document contains classified information affecting the National Defense of the United States within the meaning of the Espionage Act, USC 50:31 and 32. Its transmission or the revelation of its contents in any manner to an unauthorized person is prohibited by law. Information so classified may be imparted only to persons in the military and naval services of the United States, appropriate civilian officers and employees of the Federal Government who have a legitimate interest therein, and to United States citizens of known loyalty and discretion who of necessity must be informed thereof.

NATIONAL ADVISORY COMMITTEE FOR AERONAUTICS

WASHINGTON

June 9, 1947

NATIONAL ADVISORY COMMITTEE FOR AERONAUTICS

RESEARCH MEMORANDUM

A COMPARISON OF THREE THEORETICAL METHODS OF CALCULATING SPAN LOAD DISTRIBUTION ON SWEPT WINGS

By Nicholas H. Van Dorn and John DeYoung

SUMMARY

Three methods for calculating span load distribution, those developed by V.M. Falkner, Wm. Mutterperl, and J. Weissinger, have been applied to five swept wings. The angles of sweep ranged from -45° to $+45^{\circ}$. These methods were examined to establish their relative accuracy and ease of application. Experimentally determined loadings were used as a basis for judging accuracy. For the convenience of the readers the computing forms and all information requisite to their application are included in appendixes.

From the analysis it was found that the Weissinger method would be best suited to an over-all study of the effects of plan form on the span loading and associated characteristics of wings. The method gave good, but not best, accuracy and involved by far the least computing effort. The Falkner method gave the best accuracy but at a considerable expense in computing effort and hence appeared to be most useful for a detailed study of a specific wing. The Mutterperl method offered no advantages in accuracy or facility over either of the other methods and hence is not recommended for use.

INTRODUCTION

In an effort to reach higher flight speeds, designers are turning to widely diversified types of plan forms the aerodynamic characteristics of which are as yet unknown. Since the multiplicity of such designs precludes an experimental investigation of each, considerable attention has been directed toward means of obtaining those characteristics theoretically. Usually the basis for such theoretical investigations is span loading. While the precise span loading itself may not be considered of major importance, it is believed

that any method giving reasonably accurate predictions of span loading would be amenable to simple extensions which would give reasonably accurate values of such characteristics as lift-curve slope, spanwise center of pressure position, downwash at arbitrary locations, and rolling moments due to sideslip or rolling.

A number of methods have been developed for predicting the span loading of swept wings of arbitrary taper and aspect ratio, but very few attempts have been made to compare, for several methods, predicted and experimentally measured loadings on identical wings. The investigation reported herein was undertaken to provide such a comparison of predicted and measured span loadings. The theoretical methods have been evaluated in terms of relative accuracy, manner and consistency of error, and tediousness of application.

The methods developed by V.M. Falkner (reference 1), Wm. Muttorperl (reference 2), and J. Weissinger (reference 3) have been applied to five wings produced by sweeping the wing panels of an airplane through a range of -45° to $+45^{\circ}$ (reference 4). The span load distributions so calculated have been compared with those obtained experimentally at the time of the investigation of reference 4. In addition, the lift-curve slopes and spanwise center-of-pressure position predicted for each wing by the several methods have been compared with those values obtained experimentally.

Throughout the calculations a check was made of the time required for each method and for the various parts of each method. From these observations a comparison was made of the relative tediousness of each method, and indications were obtained as to which parts might be rendered less difficult and time consuming.

Finally, in order to enable immediate application of the methods, all necessary tables, computation forms, and step-by-step computation instructions for each are included in the appendixes. It is believed that with these aids a computing staff could undertake the computation of swept-wing characteristics with little additional supervision. In addition, for the convenience of the reader, there are included in the appendixes any mathematical derivations or developments not immediately obtainable from the references.

SYMBOLS

General

S	wing area, square feet
b	effective[1] wing span, feet
AR	effective aspect ratio (b^2/S)
s	semispan ($b/2$), feet
c	wing chord, feet
c_o	root chord, feet
c_{av}	average chord (S/b), feet
λ	taper ratio, tip chord divided by root chord (c_t/c_o)
Λ	sweep angle of quarter-chord line positive for sweepback, degrees
α	geometric angle of attack of wing measured from angle for zero lift, degrees
α_s	geometric angle of attack of wing root section, degrees
α_{local}	local geometric angle of attack, degrees
x	longitudinal coordinate of downwash point positive forward, feet
y	lateral coordinate of downwash point positive to right, feet
η	dimensionless lateral coordinate of downwash point (y/s)

[1]In all instances except the unswept wing, the actual tip chord was not parallel to the wind stream. An effective tip chord that was parallel was therefore assumed such that the wing area remained constant. The effective span is the span to this effective tip.

$\bar{x}$ longitudinal coordinate of vortex element positive forward, feet

$\bar{y}$ lateral coordinate of vortex element positive to right, feet

$\bar{\eta}$ dimensionless lateral coordinate of vortex element $(\bar{y}/s)$

c_η chord at spanwise station η, feet

ρ density of air, slugs per cubic foot

V air-stream velocity, feet per second

q air-stream dynamic pressure $(\frac{1}{2}\rho V^2)$, pounds per square foot

L lift, pounds

C_L lift coefficient (L/qS)

c_l section lift coefficient

γ vorticity, feet per second

Γ circulation, feet squared per second

η_{cp} spanwise center of pressure position

Δp differential pressure between upper and lower surfaces of wing, pounds per square foot

p static pressure, pounds per square foot

p_o free-stream static pressure, pounds per square foot

P pressure coefficient $[(p-p_o)/q]$

w induced vertical velocity or downwash, feet per second

w/V downwash angle, the ratio of downwash to free-stream velocity

φ spanwise position in circular coordinates $(\cos^{-1}\eta$ or $\cos^{-1}\bar{\eta})$

Symbols Pertaining to the Falkner Method

y_v	semispan of horseshoe vortex (s/20), feet
$x^{*\prime}$	dimensionless longitudinal coordinate (x/y_v)
x^*	dimensionless longitudinal coordinate of control point relative to vortex
x'	longitudinal coordinate referred to 0.5c line, feet
θ	circular longitudinal coordinate $(\cos^{-1} 2x'/c)$
$y^{*\prime}$	dimensionless lateral coordinate (y/y_v)
y^*	dimensionless lateral coordinate of control point relative to vortex
$a_{m,n}$	unknowns in distribution series
M	number of vortices in chordwise direction
ν	designates which of M vortices in chordwise direction
A,B,C	functions used in development
$\Gamma_{\nu,A}$; $\Gamma_{\nu,B}$; $\Gamma_{\nu,C}$	circulation increment of vortex in two-dimensional flow, feet squared per second
$G_{\nu,A}$; $G_{\nu,B}$; $G_{\nu,C}$	dimensionless circulation factors $(\Gamma_{\nu,A}/AV; \Gamma_{\nu,B}/BV; \Gamma_{\nu,C}/CV)$
Γ_ν	total circulation of vortex in two-dimensional flow, feet squared per second $(\Gamma_{\nu,A} + \Gamma_{\nu,B} + \Gamma_{\nu,C})$
μ	dimensionless lateral coordinate of midpoint of specific vortex $(\bar{y}/s)$
$\Gamma_{\nu,\mu}$	circulation of specific vortex in three-dimensional flow, feet squared per second

Λ_{LE} sweep angle of leading edge, positive for sweepback, degrees

Symbols Pertaining to the Mutterperl Method

b' dimensionless span along the 0.25c line $(b/c_o \cos \Lambda)$

s' dimensionless semispan along the 0.25c line $(b'/2)$

y' dimensionless coordinate of control point along line parallel to 0.25c line $(y/c_o \cos \Lambda)$

$\bar{y}'$ dimensionless coordinate of vortex element along 0.250c line $(\bar{y}/c_o \cos \Lambda)$

B_R, B_L perpendicular distance from 0.25c line to control point divided by c_o

A_R, A_L distance along 0.25c line from center section to base of perpendicular to control point divided by c_o

δ $A_R - y'$

ψ $\cos^{-1} y'/s'$

F $\sqrt{1 + \left[\frac{s'}{B_R}\left(\cos \varphi - \frac{A_R}{s'}\right)\right]^2}$

G $\sqrt{1 + \left[\frac{s'}{B_L}\left(\cos \varphi - \frac{A_L}{s'}\right)\right]^2}$

C $\frac{1}{B_R}\sqrt{B_R^2 + \delta^2}$

Symbols Pertaining to the Weissinger Method

ar local aspect ratio (b/c)

$G(\varphi)$ dimensionless circulation $(\Gamma(\bar{y})/bV)$ a continuous function of $\bar{\eta}$

m	number of stations at which specific circulation is to be determined and at which downwash is summed
M	number of stations at which $f_{n,\mu}$ and $L_\Lambda(\nu,\mu)$ is to be determined
n	denotes at which of m points specific circulation ordinate occurs
ν	denotes at which of m points downwash is summed
μ	denotes at which of M points $f_{n,\mu}$ or $\bar{f}_{n,\mu}$ or $L_\Lambda(\nu,\mu)$ ordinate occurs
μ_1	denotes which of m terms in interpolation function $f_{n,\mu}$
φ_n	circular coordinate of point n $(n\pi/m+1 = \cos^{-1}\bar{\eta})$
φ_ν	circular coordinate of point ν $(\nu\pi/m+1 = \cos^{-1}\eta)$
φ_μ	circular coordinate of point μ $(\mu\pi/M+1 = \cos^{-1}\eta)$
G_n	dimensionless circulation at spanwise station φ_n
G_ν	dimensionless circulation at spanwise station $\varphi_n = \varphi_\nu$
c_ν	chord at spanwise station φ_ν
ar_ν	specific local aspect ratio (b/c_ν)
$L_\Lambda(\eta,\bar{\eta})$; $L_\Lambda(\nu,\mu)$	influence function
$B_{\nu,n}$; $B^*_{\nu,n}$; B^*_ν; $b_{\nu,n}$; $b_{\nu,\nu}$; $b^*_{\nu,n}$; b^*_ν; $b^*_{\nu,\mu}$; $g_{\nu,n}$; $g_{\nu,\nu}$; $\bar{g}_{\nu,n}$; $\bar{g}_{\nu,\nu}$; t; $T(t)$; K	functions used in mathematical development
$f_{n,\mu}$; $\bar{f}_{n,\mu}$	interpolation function used in mathematical solution
β_ν	$1/ar_\nu$

DESCRIPTION OF WINGS INVESTIGATED

The five wings to which the methods have been applied are described in reference 4. Briefly, they were produced by sweeping the wing panels from an existing airplane to five angles of sweep. Each wing then consisted of a center section, the two main panels, and the two tip sections. The airfoil sections of the root and tip were generated by direct extension of the surface of the panels. The geometric characteristics of the wings are as follows:

[2]Λ	λ	AR (effective)	S
-45.2°	0.376	2.99	335.5 ft^2
-29.6°	.405	4.45	282.3 ft^2
$.9^{\circ}$	.542	4.47	201.8 ft^2
31.0°	.442	4.66	288.4 ft^2
46.4°	.418	3.45	309.5 ft^2

In all applications presented herein it was assumed that all section lift-curve slopes were 0.103 per degree, the average value of this parameter for the sections at the ends of the unswept wing panel. Actually, the local section slope varied from root to tip; however, because of the nature of the sections generated by extending the wing panels, exact values of this function could not be determined. Corrections to the theoretical methods to account for such a variation were omitted from the computations, although the effects of such an omission are discussed later.

The loading on a wing can be separated into the basic loading (that existing at zero over-all lift) which is a function of twist, camber, flap deflection, and plan form; and additional loading, which is a function of plan form and angle of attack. For purposes of analysis in this report, attention has been directed solely towards the additional loading. The wings experimentally investigated

[2]To agree with the definition of sweep used in the theoretical methods of span loading prediction, sweep has been referred to the sweep of the line joining the quarter-chord points at root and tip. In reference 4 the sweep was defined somewhat differently.

were essentially devoid of any camber or twist. Any evidence of basic loading shown by experiment was removed from the loading curves used as a basis of comparison. Thus, for purposes of analysis, the wing was replaced by a flat plate and local angles of attack become synonymous with over-all angles of attack. The characteristics of wings having camber or twist the variation of which is free from discontinuities, however, could be determined equally well by any of the methods simply by using the true local angle of attack (as measured from the angle of zero lift) at each point considered. Further discussion of this problem is given in the appendixes.

PROCEDURES

All methods described herein are extensions of simplified wing theory and so are subject to the same assumptions.

1. The fluid is incompressible.

2. The flow is potential.

3. The circulation is such that, after Kutta-Joukowski, the stagnation point occurs at the trailing edge of the airfoil.

4. The wing is represented by a thin vortex sheet in the chord plane having a plan form identical to the wing plan form.

5. All vertical displacements can be ignored. This means, for instance, that (a) when camber is introduced, the chordwise angular variation is considered but not the chordwise vertical displacement; (b) when angle of attack is considered no vertical chordwise displacements are considered; and (c) the trailing vortex sheet lies always in the same horizontal plane as the wing. This assumption strictly limits the analysis to uncambered wings at zero angle of attack; such limitations, however, can be moderately exceeded.

In replacing the wing by a vortex sheet, the strength of the vorticity γ at any point is related to the differential pressure Δp at that point by

$$\Delta p = \rho V \gamma$$

The problem of obtaining the loading, or distribution of Δp, over the wing is thus resolved into that of obtaining the strength of vorticity γ within the plan form. The control condition which is enforced to obtain the distribution of γ is that no flow can occur through the vorticity sheet, or in other words, that the downwash produced by the vorticity is proportional to the slope of the sheet at any point within its limits. The determination of γ would be exact if its distribution were considered continuous and if the foregoing condition were enforced at an infinite number of points. Such an exact determination is impractical; consequently, simplifying approximations must be introduced. The simplifications generally used are those of (1) concentrating or restricting the continuous vorticity chordwise and/or spanwise in order to make the determination of its distribution amenable to mathematical treatment; and (2) representing the distribution of vorticity or of circulation by a mathematical expression, usually a series, containing a finite number of unknown coefficients where an infinite number are generally required for exactness; and (3) limiting the number of control points at which the condition of no flow through the sheet is satisfied. The differences in the various methods developed for predicting the distribution of vorticity arise, therefore, from (1) the manner of concentrating or restricting the vorticity; (2) the differences in the form of the mathematical expressions used to describe the vorticity distributions; and (3) the choice in number and location of the control points and the precise mathematical procedure used to obtain a solution.

The Falkner Method

The wing is first considered as a continuous sheet of vorticity whose strength distribution is expressed by the double series:

$$\gamma = \frac{8s\ V \tan \alpha}{c} \sqrt{1-\overline{\eta}^2} \left[\cot \frac{\theta}{2} \left(a_{0,0} + \overline{\eta} a_{0,1} + \overline{\eta}^2 a_{0,2} \ldots\right) + \sin \theta \left(a_{1,0} + \overline{\eta} a_{1,1} + \overline{\eta}^2 a_{1,2} \ldots\right) + \sin 2\theta \left(a_{2,0} + \overline{\eta} a_{2,1} + \overline{\eta}^2 a_{2,2} \ldots\right) + \ldots a_{m,n} \overline{\eta}^n \sin m\theta \right] \tag{1}$$

in which $\overline{\eta} = \frac{\overline{y}}{s}$ and $\theta = \cos^{-1} \frac{x'}{c/2}$

Evaluation of the unknowns $a_{m,n}$ is performed in the following manner by

1. Concentrating the vorticity both chordwise and spanwise into a system of 84 finite horseshoe vortices (fig. 1(a))

2. Expressing the circulation of these vortices in terms of the unknowns in equation (1) (appendix A)

3. Summing at a number of control points on the wing the downwash produced by all the vortices of the subject system and computed by means of the Biot-Savart law

4. Equating the downwash angle thus determined to the slope of the plate at those points thereby forming equations involving the unknown coefficients

5. Solving these equations simultaneously to evaluate the coefficients $a_{m,n}$

Substitution of these values in equation (1) gives the desired expression for the load distribution.

The Mutterperl Method

Mutterperl considered only spanwise distribution of vorticity. In such an approach the chordwise distribution of vorticity is concentrated into the circulation of a lifting line. (See fig. 1(b).) The distribution of this circulation along the line is then represented by the Fourier series

$$\Gamma = 4\pi V c_o \sin \alpha \sum_{n=0}^{\infty} a_{2n+1} \sin (2n+1) \varphi \qquad (2)$$

The unknowns to be evaluated to obtain the distribution of Γ are the coefficients a_{2n+1}. The downwash produced at points on the wing by the lifting line and its trailing vortex system can be expressed in terms of these unknowns by application of the Biot-Savart law to this equation. (See appendix B.) Equating the expression for downwash angle to the slopes of the mean camber lines at these points produces a set of equations which contain the unknowns a_{2n+1}; simultaneous solution of these equations evaluates the coefficients.

The Weissinger Method

From extensions of the Multhop procedures, Weissinger developed two methods of obtaining span loading, one based on lifting surface concepts, the other on lifting line. The lifting surface method, however, amounted to little more than a substitution of the theoretical additional chordwise loading, represented by $\gamma = \text{constant} \times V \cot \frac{\theta}{2}$, for the concentrated load of the lifting-line method. According to Weissinger the surface method proved to be considerably longer, and gave results with an accuracy only slightly superior to those of the line method. For this reason, only the latter is described herein.

As in the Mutterperl method, the continuous chordwise distribution of vorticity is concentrated into the circulation of a lifting line. (See figure 1(c).) The distribution of this circulation is then specified by

$$G(\varphi) = \frac{2}{m+1} \sum_{n=1}^{m} G_n \sum_{\mu_1=1}^{m} \sin \mu_1 \varphi_n \sin \mu_1 \varphi \qquad (3)$$

The circulation $\Gamma(\bar{y})$ is represented nondimensionally as $G(\varphi)$ in this expression and the unknowns to be evaluated are G_n, the circulations at specified locations along the line. The downwash produced at points within the plan form by the lifting line and its trailing vortex system can be expressed in terms of these unknowns through application of the Biot-Savart law to equation (3). (See appendix C.) Equating the expressions for downwash angle so obtained to the slopes of the mean camber lines at these points results in a set of equations with unknowns G_n. Simultaneous solution of these equations evaluates the unknowns.

EXPERIMENTAL DATA

Pressure data were taken at a tunnel speed of 90 miles per hour which corresponds to a Reynolds number of approximately 9,000,000. Data were taken over an angle-of-attack range -3° to 9°. Plots of the chordwise distribution of pressure coefficient $P = (p-p_o)/q$ at several spanwise stations were drawn and integrated to obtain the local lift at these stations. These values of local lift were then plotted against angle of attack, and the resulting local lift-curve slopes were used to obtain the curves of the spanwise

distribution of additional load and of additional lift coefficient shown herein. The maximum error in any local lift-curve slope as the result of scatter, etc., is estimated to be 0.002 per degree. Such an error would produce a variation of the distribution curves of about one-half to one-third the magnitude of the discrepancy between the theoretically computed and the experimentally obtained curves.

RESULTS AND DISCUSSION

Comparable spanwise distributions of the loading coefficient $c_l c_\eta / C_L c_{av}$ as calculated by the three methods and as determined from the experimental surveys are presented in figure 2. Similar presentations of local lift coefficient c_l/C_L are presented in figure 3. The theoretically predicted values of lift-curve slope $dC_L/d\alpha$ and spanwise center of pressure position for the different wings are presented in table I.

From figures 2 and 3 it is apparent that all the theoretical methods tend to predict higher loadings at the center and lower loadings at the tip than were measured. In general, the Falkner method errs less in this respect than do the others. Mutterperl distribution representations for the swept-back and unswept wings are only slightly less accurate than those of Falkner. On the other hand, for the swept-forward wings the Mutterperl distributions departed from the experimental distributions to the extent that they must be considered unusable. Weissinger distribution representations were equally accurate for swept-back and swept-forward wings. The average accuracy for this method was only slightly less than that of the Falkner method.

In regard to the center of pressure position and lift-curve slope, the closest predictions in all instances were those made by the Falkner method. The Mutterperl method, in the range in which its applications may be considered usable, was also quite accurate. The Weissinger method gave good center-of-pressure positions in all instances and accurate values of lift-curve slopes in all instances except for the +45° swept wing. — 13% error from a 4-point solution.

The time studies of the calculations indicate that the Falkner method takes from 24 to 32 hours. The greater part of this time, 16 to 20 hours, is consumed in determining the values of the downwash factor F for the different vortices. The major part of the remainder is needed for the solution of the simultaneous equations, which often prove to be ill conditioned. The Mutterperl method

takes from 20 to 28 hours, the greater part of the time being consumed in the Simpson rule integration of the factors F_8' to F_8'. The Weissinger method using $m = M = 7$, takes only $2\frac{1}{2}$ to 3 hours, in which there is no phase that consumes an outstanding amount of time.

It has been stated previously that the section lift-curve slope c_{l_α} of all sections on all five wings was assumed to be 0.1030 per degree. The thickness variations from root to tip, however, indicate that variations in c_{l_α} probably exist for each wing. Unfortunately, the distortions of the sections resulting from the manner in which the wings were constructed preclude an exact determination of what the variation might be for all but the unswept wing. For this reason, the readily applicable correction to theory (see appendixes) for a variation in c_{l_α} was not included in the computations. While this correction would account at least in part for the aforementioned discrepancies between theoretical and experimental loading distributions, it should not alter the relative evaluation of the three methods.

In considering the three methods it should be noted that two of them, those of Weissinger and Mutterperl, have identical aerodynamic approaches and differ only in the mathematical procedure. It would be expected, therefore, if no compromise were made in the mathematical accuracy (i.e., if a large number of terms were used in the series), identical results would be obtained. Further, if similar limitations were impressed upon the two methods it might well be assumed that results of comparable accuracy would be obtained. The failure of the Mutterperl method to predict acceptable loadings on the swept-forward wings is inexplicable on these grounds and, as a result, must be attributed to an inconsistency introduced in the mathematical development. An additional advantage of the Weissinger method is that it lends itself to the pretabulation of a number of constants which are applicable to the solution for any plan form. It is because of this that the Weissinger method proved less time consuming than that of Mutterperl which cannot be handled in this manner. In general, then, it is apparent that the Weissinger method offers several advantages over the Mutterperl method, which, however, stem entirely from the mathematical phase of the solution. Insofar as the aerodynamic concepts are concerned neither method should be expected to be superior.

The Falkner method offers a definite aerodynamic advantage in that the wing is represented by a lifting surface rather than a lifting line. From a consideration of only the spanwise distribution of loading, the time required to use the Falkner method appears excessive when the very minor improvement in accuracy is recognized. However, if surface loading or chordwise loading were desired, the method would undoubtedly show marked superiority. The relatively long period of time required to obtain a solution by this method is in great measure a result of the large number of purely mechanical functions inherent in the method. It can be expected that such processes are amenable to handling by mechanical means if sufficient use is to be made of the method to warrant their construction. One such aid of relatively simple form has been applied in other span-loading computations using the Falkner method and resulted in cutting the computing time by 30 percent with no serious loss in accuracy. It consisted of constructing a large-scale contour chart of the downwash field around a horseshoe vortex and using this in conjunction with an appropriately scaled drawing of the wing to read directly the downwash at the various control points.

A further advantage of the Falkner method over the lifting-line methods can be seen in the increased flexibility resulting from the system of finite vortices which permit application of this method to a variety of plan forms beyond the scope of the other methods the lifting line pattern and control-point positions of which are fairly rigidly specified. In this regard, Falkner has successfully applied the method to a pterodactyl wing (reference 5) and to a wing with a parabolic 0.25c line (reference 6). It should be remembered, however, that should the plan form be of such a nature as to require a modification of the vortex lattice, the work involved will be considerably increased.

CONCLUSIONS

From the results of the subject investigation the following conclusions have been drawn:

1. Where an over-all study of the effects of sweep and plan form on span loading, lift-curve slope, etc., is desired and where good accuracy is desired for minimum effort, the Weissinger method is most useful.

2. Where a detailed study of a specific wing is desired and utmost accuracy is important even at the expense of considerable computing effort, the Falkner method should be used.

3. The Mutterperl method offered no advantages over the other methods either in terms of accuracy or facility and hence is not recommended for use.

Ames Aeronautical Laboratory,
National Advisory Committee for Aeronautics,
Moffett Field, Calif.

Nicholas H. Van Dorn,
Mechanical Engineer.

John De Young,
Physicist.

Approved:

for John F. Parsons,
Aeronautical Engineer,

TABLE I.– COMPARISON OF THEORETICAL AND EXPERIMENTAL VALUES OF LIFT-CURVE SLOPE AND SPANWISE CENTER OF PRESSURE

Wing parameters			Lift-curve slope $dc_L/d\alpha$ (deg^{-1})			
Λ	AR	λ	Falkner	Mutterperl	Weissinger	Experiment
−45.2	2.99	0.376	0.0419	0.04005	0.0450	0.0422
−29.6	4.45	.405	.0573	.0456 ?	.0585	.0580
.9	4.47	.542	.0633	.0632	.0640	.0660
31.0	4.66	.442	.0638	.0615	.0631	.0668
46.4	3.45	.418	.0509	.0495	.0470	.0538

13% error

Wing parameters			Spanwise center of pressure, η_{cp}			
Λ	AR	λ	Falkner	Mutterperl	Weissinger	Experiment
−45.2	2.99	0.376	0.398	0.385	0.399	0.401
−29.6	4.45	.405	.408	.362 ?	.403	.420
.9	4.47	.542	.429	.426	.425	.433
31.0	4.66	.442	.439	.434	.440	.444
46.4	3.45	.418	.446	.438	.442	.450

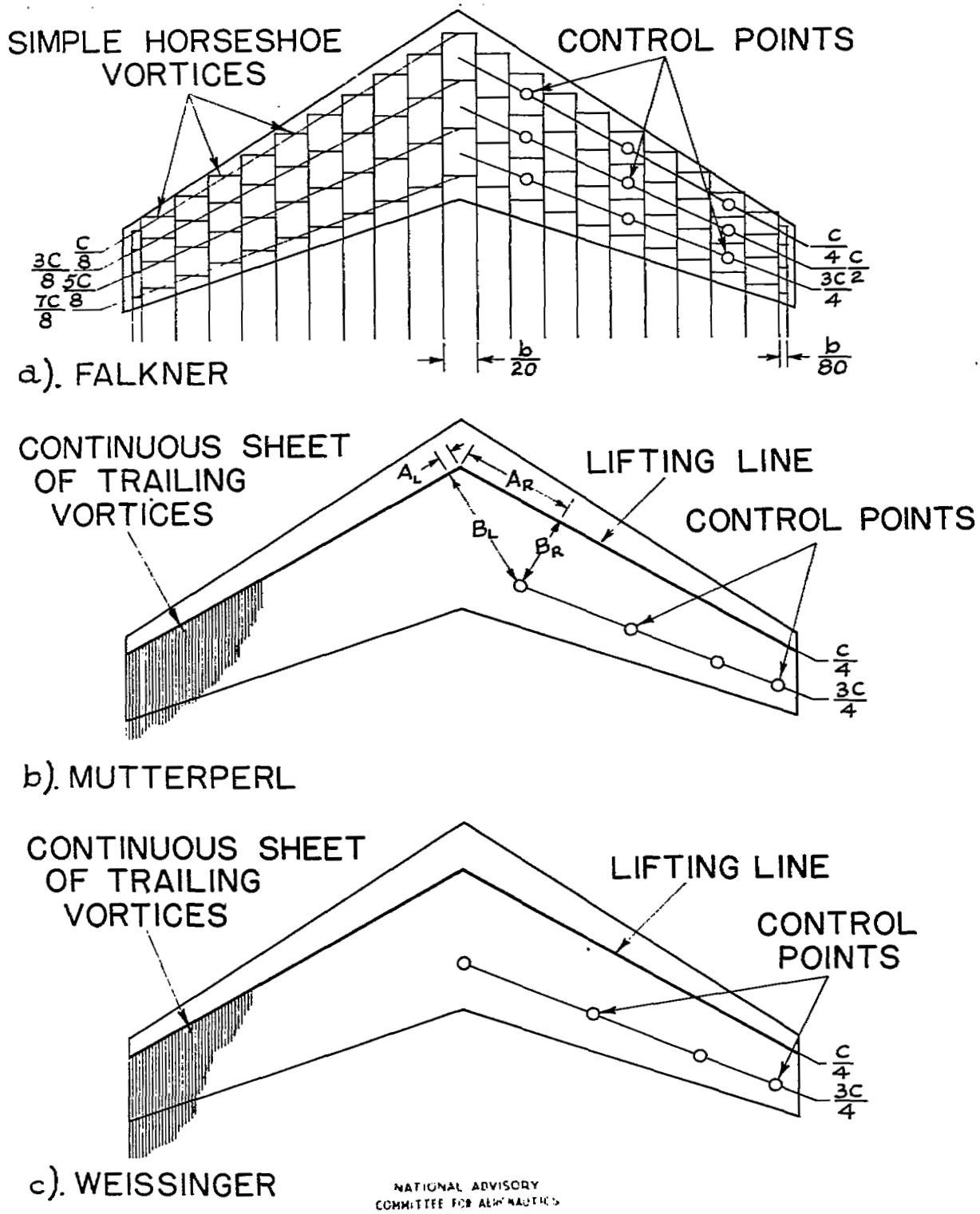

FIGURE 1. - THE MANNER OF CONCENTRATING THE VORTICITY FOR THE METHODS OF FALKNER, MUTTERPERL AND WEISSINGER.

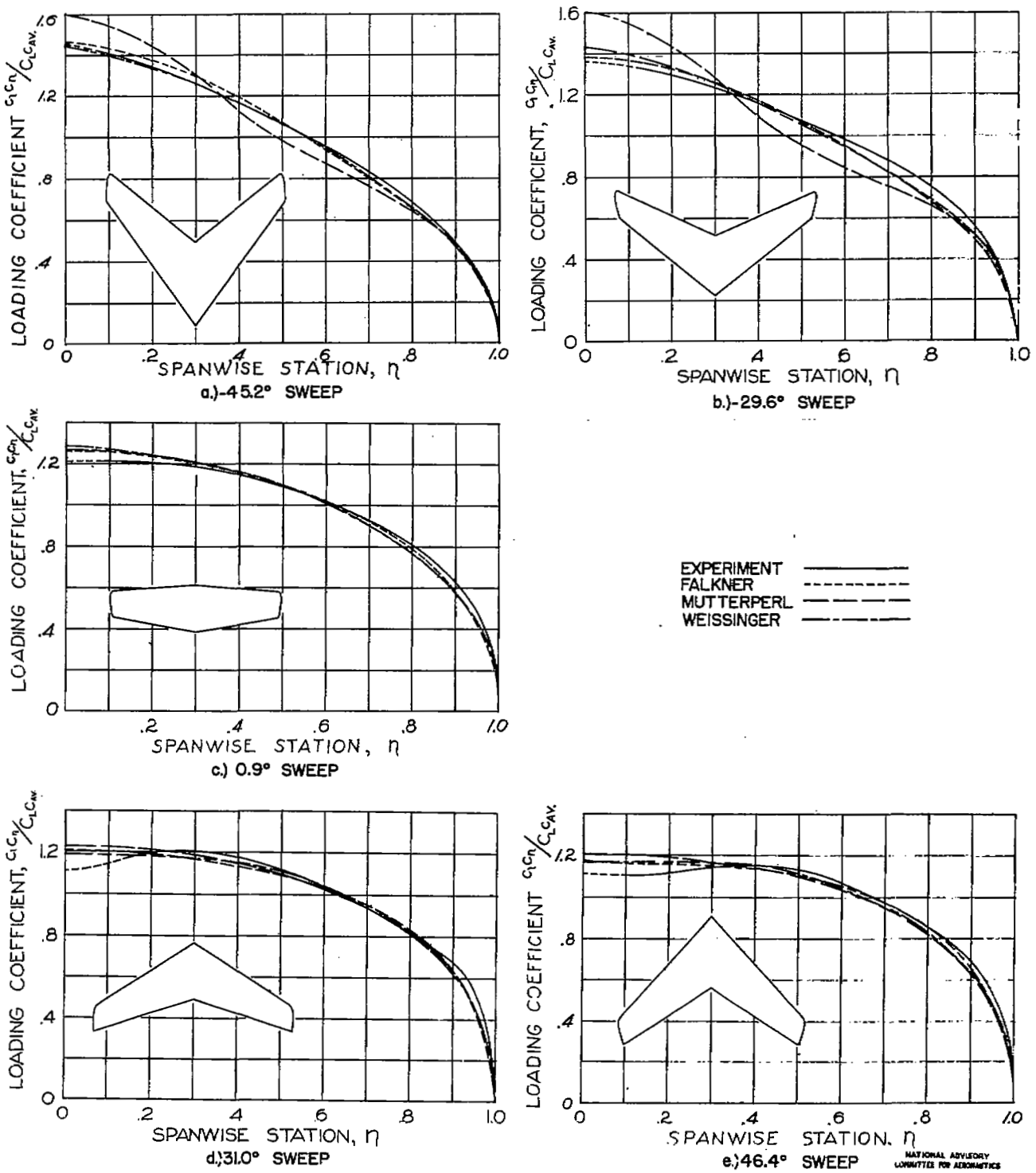

FIGURE 2.- DISTRIBUTION OF LOADING COEFFICIENT, $c_l c_n / C_L c_{av}$ ALONG THE SEMISPAN.

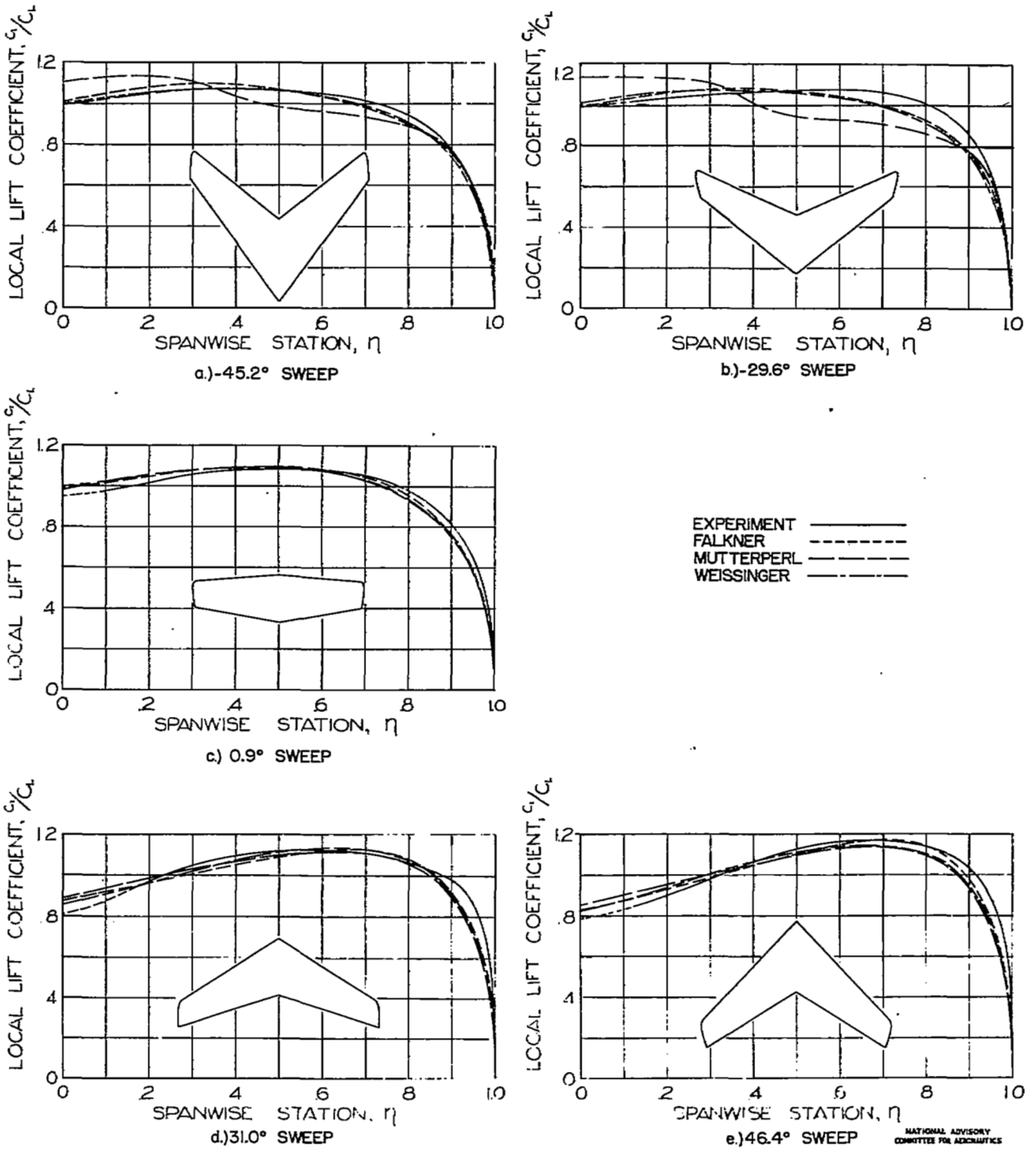

FIGURE 3.- DISTRIBUTION OF LOCAL LIFT COEFFICIENT, c_l/c_L, ALONG THE SEMISPAN.

APPENDIX A.– PERTINENT INFORMATION AND COMPUTING PROCEDURES FOR USE WITH THE FALKNER METHOD

Selection of the Vortex Pattern

The relative strength of the circulation of the vortices in a network, as expressed in terms of the unknowns in the series equation (1), depends upon the vortex pattern and the terms in the series only, not upon wing shape. Tables of such circulations can be set up for use with any specified pattern. Falkner, on the basis of his applications, selected the pattern of 84 vortices shown in figure 1(a) as suitable for most wings. While it is recognized that other patterns might produce more accurate results in particular instances, the advantages of this regular pattern in reducing the computational work are great and hence it was used for all applications included herein.

Limitations of the Series

The number of terms in equation (1) required to obtain a good approximation of the load distribution depends on the rapidity with which the series converges for each application. For the calculation of symmetrical loading, Falkner concluded that a minimum of three chordwise and three spanwise terms (nine unknowns) should be used for all swept wings, while a minimum of two spanwise and three chordwise terms (six unknowns) should be used for straight wings.

It should be recognized that, as it is given, this series will not converge when attempting to approximate a surface loading where discontinuities exist such as those resulting from partial span flaps. A slight modification to the series, however, will enable it to approximate the loading where such a discontinuity occurs. Falkner has determined the necessary modification in his investigation of wings with flaps and ailerons deflected. (See reference 7.)

Determination of Circulation of Network Vortices

Once the vortex pattern and number of terms in the basic series have been established, the circulation of the vortices as expressed in terms of the unknowns in equation (1) can be determined by replacing the continuous vorticity chordwise and spanwise of equation (1) with the concentrated stepped loading of the lattice.

The chordwise concentration of the load is determined by the condition that, at points located midway between the loads (at one-quarter, one-half, and three-quarter chord), the downwash produced by the four chordwise loads $\Gamma\gamma$ be the same as would be produced by the continuous chordwise loading in two-dimensional flow, and the limitation that the sum of the isolated loads be equal to the integral of the continuous load.

When only the first term in the chordwise series of equation (1) is considered,

$$\gamma = \frac{8sV \tan \alpha}{c}\sqrt{1-\bar{\eta}^2} \sum_{n=0}^{\infty} \bar{\eta}^n a_{o,n} \cot \frac{\theta}{2} \tag{A1}$$

or, since only chordwise loading is being considered, all factors which are not a function of the chordwise variable θ can be put into a constant A where

$$A = 8s \tan \alpha \sqrt{1-\bar{\eta}^2} \sum_{n=0}^{\infty} \bar{\eta}^n a_{o,n} \tag{A2}$$

then

$$\gamma = \frac{AV}{c} \cot \frac{\theta}{2} \tag{A3}$$

Then it can be shown that if the flow is considered two dimensional the downwash angle at any point along the chord is

$$\frac{w}{V} = \frac{1}{2}\frac{A}{c}$$

and

$$\int_{-c/2}^{c/2} \gamma dc = \frac{AV}{2}\int_0^{\pi} \cot \frac{\theta}{2} \cos \theta \, d\theta = \frac{\pi AV}{2} \tag{A4}$$

The following four equations may therefore be obtained:

$$\left.\begin{aligned}
&\Gamma_{1,A} + \Gamma_{2,A} + \Gamma_{3,A} + \Gamma_{4,A} = \frac{\pi}{2} VA && \text{(a)}\\
&8\Gamma_{1,A} - 8\Gamma_{2,A} - \frac{8}{3}\Gamma_{3,A} - \frac{8}{5}\Gamma_{4,A} = \pi VA && \text{(b)}\\
&\frac{8}{3}\Gamma_{1,A} + 8\Gamma_{2,A} - 8\Gamma_{3,A} - \frac{8}{3}\Gamma_{4,A} = \pi VA && \text{(c)}\\
&\frac{8}{5}\Gamma_{1,A} + \frac{8}{3}\Gamma_{2,A} + 8\Gamma_{3,A} - 8\Gamma_{4,A} = \pi VA && \text{(d)}
\end{aligned}\right\} \qquad \text{(A5)}$$

where equation (a) equates the integral of the continuous loading to the sum of the circulations of the separate loads, and equations (b), (c), and (d) equate the downwash at the three pivotal points as produced by the continuous loading to that produced by the four loads of Γ_ν. A simultaneous solution of these equations gives the increments of circulation of the four chordwise vortices which are equivalent to the continuous loading represented by term 1 of equation (1).

A similar solution when

$$\gamma = \frac{BV}{c} \sin \theta \qquad \text{(A6)}$$

where

$$B = 8s \tan \alpha \sqrt{1-\bar{\eta}^2} \sum_{n=0}^{\infty} \bar{\eta}^n a_{1,n} \qquad \text{(A7)}$$

gives the circulation-increment distribution which is equivalent to the continuous loading expressed by the second chordwise term of equation (1), and so forth.

The circulation[3] of a specific vortex may then be expressed by

$$\Gamma_\nu = \Gamma_{\nu,A} + \Gamma_{\nu,B} + \Gamma_{\nu,C} \ldots \tag{A8}$$

or if

$$\Gamma_{\nu,A} = AV\pi G_{\nu,A}, \quad \Gamma_{\nu,B} = BV\pi G_{\nu,B}, \quad \Gamma_{\nu,C} = CV\pi G_{\nu,C}$$

$$\Gamma_\nu = AV\pi G_{\nu,A} + BV\pi G_{\nu,B} + CV\pi G_{\nu,C} \ldots \tag{A9}$$

The substitution into this equation of the values of A, B, etc., introduces the spanwise variable $\bar{\eta}$.

$$\begin{aligned}\Gamma_{\nu,\eta} = 8\pi sV \tan\alpha \sqrt{1-\bar{\eta}^2}\,[&G_{\nu,A}\,(a_{0,0} + \bar{\eta}\,a_{0,1} + \bar{\eta}^2\,a_{0,2}\ldots) \\ &+ G_{\nu,B}\,(a_{1,0} + \bar{\eta}\,a_{1,1} + \bar{\eta}^2 a_{1,2} + \ldots) \\ &+ G_{\nu,C}\,(a_{2,0} + \bar{\eta}\,a_{2,1} + \bar{\eta}^2\,a_{2,2} + \ldots) \\ &+ \ldots]\end{aligned} \tag{A10}$$

Since the circulation of specific horseshoe vortices is now being considered, the circulation no longer varies continuously along the span but remains constant throughout the length of the bounded lines. This is equivalent to the assumption that the continuous loading is stepped at intervals equal to the length of the bounded lines of the network vortices. The continuous variable $\bar{\eta}$ of equation (1) or equation (A10) is therefore replaced in a new equation by specific values μ of $\bar{\eta}$ which indicate the midpoints of these lines. This new equation which expresses the circulation of any network vortex is then

---

[3] The values of $G_{\nu,A}$ $G_{\nu,B}$ and $G_{\nu,C}$ presented by Falkner in reference 1 were found to be in error. Under the direction of Mr. Arthur Jones these values were recomputed at Ames, and the values so obtained are presented in table A1.

$$\Gamma_{\nu,\mu} = 8\pi sV \tan\alpha\sqrt{1-\mu^2}\,[G_{\nu,A}\,(a_{0,0} + \mu\, a_{0,1} + \mu^2\, a_{0,2} + \ldots)$$
$$+ G_{\nu,B}\,(a_{1,0} + \mu\, a_{1,1} + \mu^2\, a_{1,2} + \ldots)$$
$$+ G_{\nu,C}\,(a_{2,0} + \mu\, a_{2,1} + \mu^2\, a_{2,2} + \ldots)$$
$$+ \ldots\,] \tag{A11}$$

or for a symmetrically loaded wing

$$\Gamma_{\nu,\mu} = 8\pi sV \tan\alpha\sqrt{1-\mu^2}\,[G_{\nu,A}\,(a_{0,0} + \mu^2\, a_{0,2} + \mu^4\, a_{0,4} + \ldots)$$
$$+ G_{\nu,B}\,(a_{1,0} + \mu^2\, a_{1,2} + \mu^4\, a_{1,4} + \ldots)$$
$$+ G_{\nu,C}\,(a_{2,0} + \mu^2\, a_{2,2} + \mu^4\, a_{2,4} + \ldots)$$
$$+ \ldots] \tag{A12}$$

Examination of this equation will show that, as has previously been indicated, the known parts of the equation μ, $G_{\nu,A}$, $G_{\nu,B}$, etc., are independent of wing shape. The products of these factors $\mu^n\sqrt{1-\mu^2}\,G_{\nu,A}$, $\mu^n\sqrt{1-\mu^2}\,G_{\nu,B}$, etc., have been tabulated for use in any application in which the 84-vortex pattern is used. (See table AII.)

Selection of Control Points

Since one equation is formed at each point and since there should be the same number of equations as there are unknowns, the total number of points selected is determined by the total number of unknowns retained in the series equation. Further, the spanwise and chordwise distribution of control points must correspond to the number of spanwise and chordwise terms retained in the series. The locations of the points chordwise and spanwise are limited to positions midway between or on the center line of the vortices. Aside from these limitations, the exact choice of location remains a matter of experience. Falkner found that for a calculation of symmetrical loading the arrangement presented in figure 1(a) resulted in good accuracy for wings with sweep. This arrangement has been used in all the calculations presented herein.

Determination of the Downwash

The downwash produced by a simple horseshoe vortex of circulation Γ is expressed by (reference 8)

$$\frac{w}{V} = \frac{\Gamma}{4\pi\ y_v\ V}\ F \tag{A13}$$

where

$$F = \frac{x^* - \sqrt{(x^*)^2 + (y^*+1)^2}}{x^*(y^*+1)} - \frac{x^* - \sqrt{(x^*)^2 + (y^*-1)^2}}{x^*(y^*-1)} \tag{A14}$$

The downwash produced by a network vortex is then from equations (A11), (A13), and (A14),

$$\begin{aligned}\frac{w}{V} = 40 \tan\alpha \sqrt{1-\mu^2}\ [& G_{\nu,A}\ (a_{0,0} + \mu\ a_{0,1} \ldots) \\ & + G_{\nu,B}\ (a_{1,0} + \mu\ a_{1,1} + \ldots) \\ & + G_{\nu,C}\ (a_{2,0} + \mu\ a_{2,1} + \ldots) \\ & + \ldots]\ F\end{aligned} \tag{A15}$$

or for a symmetrical wing

$$\begin{aligned}\frac{w}{V} = 40 \tan\alpha \sqrt{1-\mu^2}\ [& G_{\nu,A}\ (a_{0,0} + \mu^2\ a_{0,2} + \ldots) \\ & + G_{\nu,B}\ (a_{1,0} + \mu^2\ a_{1,2} + \ldots) \\ & + G_{\nu,C}\ (a_{2,0} + \mu^2\ a_{2,2} + \ldots) \\ & + \ldots]\ F\end{aligned} \tag{A16}$$

The coordinates x^*, y^*, and consequently the factor F can be determined readily from wing geometry. In this regard, plots of the function F versus x^* from 0 to 20 have been prepared at values of $y^* = 0, 2, 4, 6 \ldots 40$; however because of their size these

charts as such have not been included in the report, but the tabular data necessary for their construction are given in table AIII. In addition, examination of (A14) will reveal that if y^* is constant

$$F(-x^*) = F_1 + F_2 - F(x^*) \tag{A17}$$

where $F_1 + F_2$ is a function of y^* only

$$F_1 + F_2 = \frac{2}{y^*+1} - \frac{2}{y^*-1} \tag{A18}$$

For this reason table AIII contains only positive values of x^*, and the function $F_1 + F_2$ is presented in table AIV.

Summation of the downwash at any control point now results in an expression containing the unknowns $a_{m,n}$ and their numerical coefficients which are products of the tabulated values $\mu^n\sqrt{1-\mu^2}$, $G_{\nu,A}$, $G_{\nu,B}$, $G_{\nu,C}$, and F. In this regard it should be noted that in the summations for a symmetrical (about root chord) wing, the downwash factors F for symmetrically located vortices may be added together prior to the multiplication of these factors by the circulations of the vortices, since in this instance the circulation of such a pair of vortices will be identical.

Solution for Additional Loading

To obtain the additional loading, the wing is considered a flat plate the slope at which any point is $\tan\alpha = \frac{w}{V}$. Substitution of this value into the downwash expressions, as evaluated at the several control points, results in a set of equations with unknowns $a_{m,n}$. Simultaneous solution of these equations evaluates the unknowns which can then be introduced into equation (1) to produce the desired expression for additional loading.

The following expressions can now be derived readily from equation (1):

$$\frac{dC_L}{d\alpha} = \frac{AR\,\pi^2}{16}\left(16a_{0,0}+8a_{1,0}+4a_{0,2}+2a_{1,2}+2a_{0,4}+a_{1,4}\right) \tag{A19}$$

$$\frac{c_l}{C_L} = \frac{(1+\lambda)\,16\sqrt{1-\bar{\eta}^2}\,\left[2a_{0,0}+a_{1,0}+\bar{\eta}^2(2a_{0,2}+a_{1,2})+\bar{\eta}^4(2a_{0,4}+a_{1,4})\right]}{\pi\left[1-(1-\lambda)\bar{\eta}\right]\left(16a_{0,0}+8a_{1,0}+4a_{0,2}+2a_{1,2}+2a_{0,4}+a_{1,4}\right)} \tag{A20}$$

$$\frac{c_l\ c_\eta}{C_L\ c_{av}} = \frac{32\sqrt{1-\bar{\eta}^2}\ [2a_{0,0}+a_{1,0}+\bar{\eta}^2(2a_{0,2}+a_{1,2})+\bar{\eta}^4(2a_{0,4}+a_{1,4})]}{\pi(16a_{0,0}+8a_{1,0}+4a_{0,2}+2a_{1,2}+2a_{0,4}+a_{1,4})} \qquad \text{(A21)}$$

$$\eta_{cp} = \frac{32\ [35(2a_{0,0}+a_{1,0})+14(2a_{0,2}+a_{1,2})+8(2a_{0,4}+a_{1,4})]}{105\pi(16a_{0,0}+8a_{1,0}+4a_{0,2}+\ 2a_{1,2}+2a_{0,4}+a_{1,4})} \qquad \text{(A22)}$$

into which the coefficients $a_{m,n}$, must be substituted to obtain the quantities indicated.

Solution for Basic Loading

The determination of the basic loading on a wing with camber and twist can be accomplished in several ways. The simplest of these is to calculate the total loading, basic plus additional, at some finite lift coefficient and then to subtract from this the additional loading as calculated for that lift coefficient. A solution for the total loading on a cambered and twisted wing is identical with that of a flat-plate wing up to the formation of the simultaneous equations. For the flat-plate wing all local geometric angles of attack were identical to the wing geometric angle of attack; in this instance local geometrical angles of attack are in addition a function of the camber and twist.

If the midwing section of the wing is chosen as a reference and set arbitrarily at some angle α_s, then the local geometrical angles of attack at the various control points are known exactly; however, the angle α of the reference from the zero lift angle of the wing is not known. To obtain a solution under these circumstances the values $\tan \alpha_{local}$ and $\tan \alpha_s$ are substituted for w/V and $\tan \alpha$, respectively, in the downwash expressions, and a solution for the coefficients $a_{m,n}$ is obtained in which, however, these coefficients will be in error by the factor $\tan \alpha/\tan \alpha_s$. If these coefficients and the factor $\tan \alpha$ are then introduced into the expression for lift coefficient.

$$C_L = \frac{\pi^2 AR}{16} \tan \alpha(16a_{0,0}+8a_{1,0}+4a_{0,2}+2a_{1,2}+2a_{0,4}+a_{1,4}) \qquad \text{(A23)}$$

the lift coefficient for the angle of attack α will be obtained, since the error introduced by using α_s will be negated by the error in the coefficients $a_{m,n}$. In other words, the result is the same as if the correct values of $a_{m,n}$ and $\tan \alpha$ had been inserted into

equation (A23). Similarly introduction of $\tan \alpha_s$ and the incorrect values of $a_{m,n}$ into the following:

$$c_l c_\eta = 4\pi s \tan \alpha \sqrt{1-\overline{\eta}^2}\ [2a_{0,0}+a_{1,0}+\overline{\eta}^2(2a_{0,2}+a_{1,2})+\overline{\eta}^4(2a_{0,4}+a_{1,4})] \tag{A24}$$

will result in the values of the ordinates of the total loading curve for $\tan \alpha$ Now if a solution is effected for the additional loading, as previously described, and the value of the lift-curve slope $dC_L/d\alpha$ thus obtained from equation (A19) is divided into the value of C_L obtained from equation (A23), the correct value of the wing angle of attack $\tan \alpha$ will result. If this value and the coefficients $a_{m,n}$ of the additional loading are then substituted into expression (A24), the ordinates of the additional loading curve will be obtained. Subtraction of these from the ordinates of the total loading curve will result in the ordinates of the desired basic loading curve.

Correction for Section Lift-Curve Slope

Through the general development of the method all section lift-curve slopes were assumed to be the theoretical 2π per radians (0.1096 per deg). As this assumption is not valid for all sections the final expression for vorticity will be in error unless a correction is applied. If the section lift-curve slope is the same at all sections of the wing, the error may be corrected by simply multiplying each coefficient $a_{m,n}$ by the ratio of actual section lift-curve slope to theoretical section lift-curve slope. A varying section lift-curve slope can be accommodated almost as easily; however, in this instance the correction must be introduced into equation (1) as a function of the spanwise variable $\overline{\eta}$.

Computing Instructions

The following instructions apply to unyawed straight tapered swept wings without camber or twist.

The coordinates $x^{*\prime}$ and $y^{*\prime}$ relating all vortices and control points to the center section leading edge of the wing are calculated on form A(1) using the relations

$$y^{*\prime} = 20\ \mu$$

$$x^{*\prime} = 20\ |\mu| \tan \Lambda - \frac{80\nu}{(1+\lambda)AR}\ [1 - (1-\lambda)\ |\mu|] \tag{A25}$$

for the vortices, and

$$y^{*\prime} = 20\ \overline{\eta}$$

$$x^{*\prime} = 20\ |\overline{\eta}| \tan \Lambda - \frac{80\nu}{(1+\lambda)AR}\ [1 - (1-\lambda)\ |\overline{\eta}|] \tag{A26}$$

for the control points. Since the wing is symmetrical $x^{*\prime}$ will be the same for similarly located vortices on each wing half, and the values of $y^{*\prime}$ for the left wing will be the same as those for the right wing, although of opposite sign. For this reason these values only need be computed for positive values of $\overline{\eta}$ or μ.

The values of x^* and y^* relating a control point to each of the vortices are obtained by subtracting the values of $x^{*\prime}$ and $y^{*\prime}$ of the vortices from those of the control point, column 9 or 3, form A(1) from a value in column 18 or 12, form A(1), respectively; x^* and y^* are then tabulated on a form A(2), using a separate form for each control point. It should be noted that since the coordinates of the vortices at $\mu = 0.9625$ are based upon a unit length y_v one-quarter normal size, x^* and y^* for these vortices are four times the normally calculated values. Lastly, by virtue of symmetry of plan form, the coordinates can be tabulated so that two values $y_L{}^*$ and $y_R{}^*$ exist for every value of x^*.

These coordinates are now used to enter charts of the downwash function F as prepared from the values in table AIII. The values obtained for the vortices at $\mu = 0.9625$ should be multiplied by four. Because of symmetry of loading, F_R and F_L can be and are added together.

The simultaneous equations set up in tabular form in form A(3) are now obtained as follows: Considering the first equation or column 1, the second number, the numerical coefficient of $a_{0,0}$, is obtained by multiplying the values of $F_R + F_L$ in column 7, form A(2) as determined for control point 1 by the values listed under $a_{0,0}$ in table AII and summing the products. Similarly, the third number in column 1, the numerical coefficient of $a_{1,0}$, is obtained by multiplying the values in column 7 by the values

listed under $a_{1,0}$ in table AII and summing the product. The process is repeated using the values listed under $a_{2,0}$, $a_{0,2}$, etc., until the entire equation is obtained.

The second equation, column 2, form A(3), is set up in the same manner except that the values in form A(2) as determined for a second control point are used. The procedure is then repeated until the nine required equations are formed.

The constant numbers, row 1 of form A(3), are obtained as follows: The downwash at control point 1 is

$$\frac{w}{V} = 40 \tan \alpha \times \text{column 1, form A(3)}$$

or

$$\left(\frac{w/V}{\tan \alpha}\right) \left(\frac{1}{40}\right) = \text{column 1, form A(3)}$$

Equating $\frac{w}{V}$ to the slope of the plate, $\tan \alpha$,

$$\frac{1}{40} = 0.0250 = \text{column 1, form A(3)}$$

In like manner the constants for the other equations are also 0.0250.

The equations are set up in this manner to facilitate their solution by the method outlined in reference 9. Of the various methods for solving a large number of simultaneous equations which were tried, the method of reference 9 was found to be most rapid and straightforward where only standard computing machines were available.

$\Lambda_{L.E.} = -40°35'$ $\tan\Lambda_{L.E.} = -.85660$ $\lambda = .376$ $(1-\lambda) = .624$ $AR = 2.99$

1	2	3	4	5	6	7	8	9	10	11	12	13	14	15	16	17	18
ν	μ	20×(2)	−(3) ×tanΛ	$\frac{-80(1)}{(1+\lambda)AR}$	(2)×(1−λ)	1−(6)	(7)×(5)	(4) + (8)	ν	η	20×(11)	−(12) ×tanΛ	$\frac{-80(10)}{(1+\lambda)AR}$	(11)×(1−λ)	1−(15)	(16)×(14)	(13) + (17)
.125	0	0	0	$\bar{2}.43058$	0	1.00000	$\bar{2}.43058$	$\bar{2}.43058$	1/4	.2	4.0	3.43640	$\bar{4}.86119$	.1248	.8752	$\bar{3}.39980$	$\bar{2}.82810$
	.1									.5							
	.2									.8							
	.3								1/2	.2							
	.4									.5							
	.5									.8							
	.6																
	.7																
	.8																
	.9																
	.9625																
.375																	

(1.)

Control Point – 1

$x^{*1} = -2.43058$ $y^{*1} = 0$

1	2	3	4	5	6	7
vortex ν, μ	x^*	y_R^*	y_L^*	F_R	F_L	(6) + (5)
.125, 0	1.604	4	—	−.0810	—	−.0810
.1						
.2						
.3						
.4						
.5						
.6						
.7						

(2.)

NATIONAL ADVISORY COMMITTEE FOR AERONAUTICS

FORM A:– COMPUTING FORM FOR FALKNER'S METHOD
(Underscored numbers are sample calculations)

Equation	1	2	3	4	5	6	7	8	9	$a_{m,n}$
constant	.0250	.0250	.0250	.0250	.0250	.0250	.0250	.0250	.0250	
$a_{0,0}$	.202150									.104962
$a_{1,0}$	.207180									-.014664
$a_{2,0}$	.226410									-.141448
$a_{0,2}$	.301260									.007216
$a_{1,2}$	.304890									.142279
$a_{2,2}$	.309030									-.013880
$a_{0,4}$	.358100									.146166
$a_{1,4}$	.365820									-.189951
$a_{2,4}$	.363090									-.002979

(3.)

FORM A:- CONCLUDED

NATIONAL ADVISORY
COMMITTEE FOR AERONAUTICS

TABLE AI.- CHORDWISE FACTORS G FOR VORTEX PATTERN UTILIZING FOUR CHORDWISE VORTICES

ν	$G_{\nu,A}$	$G_{\nu,B}$	$G_{\nu,C}$
0.125	0.27337	0.04902	0.07282
.375	.11680	.07598	.03823
.625	.06947	.07598	-.03823
.875	.04036	.04902	-.07282

TABLE AII.- PRODUCT OF CHORDWISE AND SPANWISE FACTORS FOR $a_{m,n}$ TO BE USED WITH THE 84-VORTEX PATTERN SYMMETRICAL LOADING

NATIONAL ADVISORY COMMITTEE FOR AERONAUTICS

ν	μ	$\sqrt[4]{1-\mu^2} \times G_{\nu,A}$ for $a_{0,0}$	$\sqrt[4]{1-\mu^2} \times G_{\nu,B}$ for $a_{1,0}$	$\sqrt[4]{1-\mu^2} \times G_{\nu,C}$ for $a_{2,0}$	$\mu^2\sqrt[4]{1-\mu^2} \times G_{\nu,A}$ for $a_{0,2}$	$\mu^2\sqrt[4]{1-\mu^2} \times G_{\nu,B}$ for $a_{1,2}$	$\mu^2\sqrt[4]{1-\mu^2} \times G_{\nu,C}$ for $a_{2,2}$	$\mu^4\sqrt[4]{1-\mu^2} \times G_{\nu,A}$ for $a_{0,4}$	$\mu^4\sqrt[4]{1-\mu^2} \times G_{\nu,B}$ for $a_{1,4}$	$\mu^4\sqrt[4]{1-\mu^2} \times G_{\nu,C}$ for $a_{2,4}$
0.125	0	0.27337	0.04902	0.07282	0	0	0	0	0	0
	.1	.27200	.04877	.07246	.00271	.00049	.00072	.00003	0	.00001
	.2	.26785	.04803	.07135	.01072	.00192	.00285	.00044	.00008	.00012
	.3	.26077	.04676	.06947	.02348	.00421	.00626	.00210	.00038	.00056
	.4	.25054	.04493	.06674	.04008	.00719	.01068	.00642	.00115	.00171
	.5	.23674	.04245	.06306	.05918	.01061	.01577	.01479	.00256	.00394
	.6	.21870	.03922	.05826	.07873	.01412	.02097	.02835	.00508	.00755
	.7	.19521	.03501	.05200	.09565	.01715	.02548	.04688	.00841	.01249
	.8	.16402	.02941	.04369	.10497	.01882	.02796	.06719	.01205	.01790
	.9	.11916	.02137	.03174	.09653	.01731	.02571	.07818	.01402	.02083
	.9625	.07417	.01330	.01976	.06870	.01232	.01830	.06364	.01141	.01695
.375	0	.11680	.07598	.03823	0	0	0	0	0	0
	.1	.11622	.07560	.03804	.00116	.00075	.00038	.00001	.00001	0
	.2	.11444	.07445	.03746	.00458	.00298	.00150	.00019	.00012	.00006
	.3	.11142	.07248	.03647	.01003	.00653	.00328	.00090	.00059	.00029
	.4	.10705	.06964	.03504	.01712	.01114	.00560	.00274	.00179	.00090
	.5	.10115	.06580	.03311	.02529	.01645	.00828	.00632	.00411	.00207
	.6	.09344	.06078	.03058	.03364	.02188	.01101	.01211	.00788	.00396
	.7	.08341	.05426	.02730	.04087	.02659	.01338	.02003	.01303	.00656
	.8	.07008	.04559	.02294	.04485	.02918	.01468	.02871	.01868	.00940
	.9	.05091	.03312	.01666	.04124	.02683	.01350	.03340	.02173	.01093
	.9625	.03169	.02061	.01037	.02934	.01909	.00961	.02709	.01769	.00890
.625	0	.06947	.07598	-.03823	0	0	0	0	0	0
	.1	.06912	.07560	-.03804	.00069	.00075	-.00038	.00001	.00001	0
	.2	.06807	.07445	-.03746	.00272	.00298	-.00150	.00011	.00012	-.00006
	.3	.06627	.07248	-.03647	.00597	.00653	-.00328	.00053	.00059	-.00029
	.4	.06367	.06964	-.03504	.01018	.01114	-.00560	.00163	.00179	-.00090
	.5	.06016	.06580	-.03311	.01504	.01645	-.00828	.00376	.00411	-.00207
	.6	.05558	.06078	-.03058	.02001	.02188	-.01101	.00720	.00788	-.00396
	.7	.04961	.05426	-.02730	.02431	.02659	-.01338	.01191	.01303	-.00656
	.8	.04168	.04559	-.02294	.02668	.02918	-.01468	.01708	.01868	-.00940
	.9	.03028	.03312	-.01666	.02453	.02683	-.01350	.01987	.02173	-.01093
	.9625	.01885	.02061	-.01037	.01746	.01909	-.00961	.01617	.01769	-.00890
.875	0	.04036	.04902	-.07282	0	0	0	0	0	0
	.1	.04016	.04877	-.07246	.00040	.00044	-.00072	0	0	-.00001
	.2	.03954	.04803	-.07135	.00158	.00192	-.00285	.00006	.00008	-.00012
	.3	.03850	.04676	-.06947	.00347	.00421	-.00626	.00031	.00038	-.00056
	.4	.03699	.04493	-.06674	.00592	.00719	-.01068	.00095	.00115	-.00171
	.5	.03495	.04245	-.06306	.00874	.01061	-.01577	.00218	.00265	-.00394
	.6	.03229	.03922	-.05826	.01162	.01412	-.02097	.00419	.00508	-.00755
	.7	.02882	.03501	-.05200	.01412	.01715	-.02548	.00692	.00841	-.01249
	.8	.02422	.02941	-.04369	.01550	.01882	-.02796	.00992	.01205	-.01790
	.9	.01759	.02137	-.03174	.01425	.01731	-.02571	.01154	.01402	-.02083
	.9625	.01095	.01330	-.01976	.01014	.01232	-.01830	.00940	.01141	-.01695

TABLE AIII.– DOWNWASH FACTOR F IN THE FIELD OF A HORSESHOE VORTEX
[At positive values of x* only]

x*	F + (2/x)	F									
	y* = 0	y* = 2	y* = 4	6	8	10	12	14	16	18	20
0	2.00000	–.66667	–.13333	–.05714	–.03175	–.02020	–.01399	–.01025	–.00785	–.00619	–.00502
.1	1.90020	–.62234	–.12976	–.05616	–.03135	–.01999	–.01387	–.01018	–.00780	–.00616	–.00499
.2	1.80200	–.57875	–.12625	–.05519	–.03093	–.01980	–.01375	–.01011	–.00774	–.00612	–.00497
.3	1.70647	–.53652	–.12271	–.05421	–.03053	–.01959	–.01364	–.01003	–.00770	–.00609	–.00493
.4	1.61484	–.49621	–.11920	–.05326	–.03011	–.01938	–.01352	–.00996	–.00765	–.00605	–.00491
.5	1.52788	–.45819	–.11573	–.05226	–.02973	–.01919	–.01340	–.00988	–.00760	–.00602	–.00489
.6	1.44603	–.42269	–.11228	–.05130	–.02934	–.01897	–.01329	–.00981	–.00755	–.00599	–.00486
.7	1.36954	–.38981	–.10889	–.05034	–.02893	–.01878	–.01317	–.00974	–.00750	–.00595	–.00484
.8	1.29844	–.35957	–.10555	–.04938	–.02854	–.01857	–.01305	–.00967	–.00745	–.00592	–.00481
.9	1.23254	–.33186	–.10227	–.04843	–.02814	–.01838	–.01293	–.00959	–.00740	–.00589	–.00478
1.0	1.17158	–.30655	–.09904	–.04750	–.02774	–.01817	–.01282	–.00952	–.00736	–.00584	–.00476
1.5	.92963	–.21017	–.08400	–.04292	–.02581	–.01718	–.01224	–.00915	–.00711	–.00568	–.00464
2.0	.76393	–.14956	–.07093	–.03863	–.02394	–.01620	–.01167	–.00880	–.00686	–.00551	–.00451
2.5	.64594	–.11032	–.05986	–.03468	–.02214	–.01526	–.01112	–.00844	–.00663	–.00534	–.00439
3.0	.55849	–.08398	–.05066	–.03107	–.02045	–.01435	–.01057	–.00810	–.00639	–.00517	–.00427
4	.43845	–.05255	–.03683	–.02492	–.01739	–.01264	–.00953	–.00743	–.00593	–.00485	–.00403
6	.30574	–.02555	–.02100	–.01632	–.01255	–.00974	–.00770	–.00620	–.00508	–.00423	–.00357
8	.23444	–.01489	–.01318	–.01112	–.00918	–.00752	–.00620	–.00515	–.00433	–.00367	–.00314
10	.19012	–.00969	–.00893	–.00791	–.00685	–.00587	–.00500	–.00428	–.00367	–.00318	–.00277
15	.12889	–.00438	–.00422	–.00397	–.00368	–.00335	–.00305	–.00274	–.00247	–.00223	–.00200
20	.09750	–.00248	–.00243	–.00234	–.00223	–.00211	–.00199	–.00185	–.00171	–.00157	–.00148

TABLE AIII.- Concluded.

x*	F									
	y* 22	24	26	28	30	32	34	36	38	40
0	-.00413	-.00348	-.00296	-.00256	-.00222	-.00196	-.00173	-.00154	-.00139	-.00125
.1	-.00412	-.00346	-.00295	-.00255	-.00221	-.00195	-.00172	-.00154	-.00139	-.00125
.2	-.00410	-.00345	-.00294	-.00254	-.00220	-.00195	-.00172	-.00154	-.00138	-.00124
.3	-.00409	-.00343	-.00293	-.00253	-.00219	-.00194	-.00171	-.00153	-.00138	-.00124
.4	-.00407	-.00342	-.00291	-.00252	-.00218	-.00193	-.00171	-.00153	-.00137	-.00123
.5	-.00405	-.00340	-.00290	-.00251	-.00218	-.00192	-.00170	-.00152	-.00137	-.00123
.6	-.00403	-.00338	-.00289	-.00250	-.00217	-.00192	-.00170	-.00152	-.00137	-.00123
.7	-.00401	-.00337	-.00288	-.00249	-.00217	-.00191	-.00170	-.00151	-.00136	-.00122
.8	-.00400	-.00336	-.00287	-.00248	-.00216	-.00190	-.00169	-.00151	-.00136	-.00122
.9	-.00398	-.00334	-.00286	-.00247	-.00215	-.00190	-.00168	-.00150	-.00136	-.00122
1.0	-.00396	-.00333	-.00285	-.00246	-.00215	-.00190	-.00168	-.00150	-.00135	-.00122
1.5	-.00387	-.00325	-.00279	-.00242	-.00211	-.00186	-.00166	-.00148	-.00134	-.00120
2.0	-.00377	-.00318	-.00273	-.00237	-.00208	-.00183	-.00163	-.00146	-.00132	-.00118
2.5	-.00368	-.00311	-.00268	-.00233	-.00204	-.00180	-.00161	-.00144	-.00130	-.00117
3.0	-.00358	-.00304	-.00263	-.00228	-.00200	-.00177	-.00158	-.00142	-.00128	-.00115
4	-.00339	-.00291	-.00251	-.00219	-.00193	-.00172	-.00153	-.00137	-.00124	-.00113
6	-.00305	-.00263	-.00230	-.00201	-.00179	-.00160	-.00143	-.00129	-.00117	-.00106
8	-.00273	-.00237	-.00209	-.00186	-.00165	-.00148	-.00133	-.00121	-.00110	-.00101
10	-.00242	-.00214	-.00190	-.00170	-.00152	-.00137	-.00124	-.00113	-.00103	-.00095
15	-.00180	-.00164	-.00148	-.00134	-.00123	-.00113	-.00103	-.00095	-.00088	-.00081
20	-.00135	-.00125	-.00116	-.00106	-.00099	-.00092	-.00086	-.00079	-.00074	-.00069

TABLE AIV.- AUXILIARY FUNCTION $F_1 + F_2$ FOR DETERMINING DOWNWASH FUNCTION F AT NEGATIVE VALUES OF x*
$[F(-x^*) = F_1 + F_2 - F(+x^*)]$

y*	$F_1 + F_2$	y*	$F_1 + F_2$
0	4.0000	24	-0.0070
2	-1.3333	26	-.0059
4	-.2667	28	-.0051
6	-.1143	30	-.0044
8	-.0635	32	-.0039
10	-.0404	34	-.0035
12	-.0280	13	-.02381
14	-.0205	37	-.00292
16	-.0157	61	-.00108
18	-.0124	93	-.00046
20	-.0100	117	-.00029
22	-.0083	141	-.00020

APPENDIX B.– PERTINENT INFORMATION AND COMPUTING PROCEDURES FOR USE WITH THE MUTTERPERL METHOD

A lifting line used to represent a wing is placed in a position corresponding to the quarter-chord line of the wing. The distribution of circulation along the lifting line is expressed by equation (2).

No generalization can be made as to the number of terms which must be retained in the series to ensure acceptable accuracy. Mutterperl implies that four are sufficient and utilizes this number in all applications. It should be noted that all loadings predicted by the series as it stands will be symmetrical. In addition, equation (2) cannot satisfactorily approximate a curve containing discontinuities such as would be produced by flaps or ailerons. Mutterperl made no comment as to additions or alterations to the series which would enable circumvention of these limitations. As a result, while it is believed that such modifications could be included, it is not known to what extent they would increase the complexity of the mathematical evaluation.

Since it can be shown that in a theoretical approach using a lifting line at the quarter-chord line, the downwash angle at the three-quarter-chord line most closely approximates the true angle of attack of the wing, the control points were placed along this line. The number of points required is dictated by the number of unknown coefficients retained in equation (3). The location of these points spanwise is apparently arbitrary; however, since Mutterperl placed them on the right wing half at $\eta = 0.174$, 0.500, 0.766, 0.940 ($\psi = 80^\circ$, 60°, 40°, 20°), this arrangement has been followed in all applications presented herein.

Determination of Downwash

The expression for downwash at a control point, as determined through the Biot-Savart relation, is

$$\frac{w/V}{\sin\alpha} = \sum_{n=0}^{3} (2n+1)a_{2n+1}\left\{\frac{(-1)^n}{2n+1}\left(\frac{A_R}{B_R\sqrt{A^2_R+B^2_R}} - \frac{A_L}{B_L\sqrt{A^2_L+B^2_L}}\right)\right.$$

$$+ \frac{\pi}{s'\cos\Lambda}\frac{\sin(2n+1)\psi}{\sin\psi} + \frac{s'}{B^2_R}\int_0^{\pi/2}\frac{\cos(2n+1)\varphi\cos\varphi d\varphi}{F}$$

$$-\frac{1}{B_R}\left(\frac{A_R}{B_R}+\tan\Lambda\right)\int_0^{\pi/2}\frac{\cos(2n+1)\varphi d\varphi}{F} + \frac{1}{s'C}\left(1+\frac{A_R-y'}{B_R}\tan\Lambda\right)$$

$$\times\left[K_{2n+1} - \left(\frac{s'}{B_R}\right)\int_0^{\pi/2}\frac{\cos(2n+1)\varphi\left(\cos\varphi - \frac{y'+2\delta}{s'}\right)d\varphi}{F(C+F)}\right]$$

$$+\frac{s'}{B^2_L}\int_0^{\pi/2}\frac{\cos\varphi\cos(2n+1)\varphi d\varphi}{G} + \frac{1}{B_L}\left(\frac{A_L}{B_L}-\tan\Lambda\right)\int_0^{\pi/2}\frac{\cos(2n+1)\varphi d\varphi}{G}$$

$$\left.+\frac{1}{s'}\left(1-\frac{(A_L-y')\tan\Lambda}{B_L}\right)\int_0^{\pi/2}\frac{\cos(2n+1)\varphi d\varphi}{\cos\varphi+\frac{n'}{s'}G}\right\} \qquad \text{(B1)}$$

Equation (B1) may be reduced to a simple expression, containing only the unknowns a_{2n+1} and their numerical coefficients simply by the introduction of wing geometry and the geometry of a control point. Such a reduction should therefore be carried out at each of the points.

Solution for Additional Loading

Since for such a solution the wing is considered a flat plate, all geometric angles of attack become $\sin\alpha$ and the constant factors in equation (B1) become one. Simultaneous solution of these equations then evaluates the unknowns a_{2n+1}, which are subsequently introduced into equation (2) to produce the desired expression for additional loading. The unknowns can also be introduced into the following expressions derived from equation (2), to obtain the values indicated.

$$\frac{dC_L}{d\alpha} = \frac{2\pi^2 bC_o}{S} a_1 = \frac{4\pi^2 a_1}{1+\lambda} \tag{B2}$$

$$\frac{c_l}{C_L} = \frac{2(1+\lambda)}{\pi a_1[1-(1-\lambda)\cos\varphi]} (a_1 \sin\varphi + a_3 \sin 3\varphi + a_5 \sin 5\varphi + a_7 \sin 7\varphi) \tag{B3}$$

$$\frac{c_l c_\eta}{C_L\, c_{av}} = \frac{4}{\pi a_1} (a_1 \sin\varphi + a_3 \sin 3\varphi + a_5 \sin 5\varphi + a_7 \sin 7\varphi) \tag{B4}$$

$$\eta_{cp} = \frac{4}{3\pi}\left(1 + \frac{3a_3}{5a_1} - \frac{a_5}{7a_1} + \frac{a_7}{15a_1}\right) \tag{B5}$$

Solution for Basic Loading

As in Falkner, the basic loading on a twisted and/or cambered airfoil can best be calculated by determining the total and additional loading at some finite lift coefficient and subtracting the latter from the former. The procedures involved are parallel to those of the Falkner method as well. An arbitrary angle of attack α_s can be selected for the root section of the wing, from which all local angles of attack can be measured. Substitution of $\sin\alpha_{local}$ for w/V and $\sin\alpha_s$ for $\sin\alpha$ in the expression (B1) will result in a set of equations which may be solved simultaneously for the values of the coefficients a_{2n+1}. If a_1 and $\sin\alpha_s$ are are then introduced into the following, the correct value of the lift coefficient for the wing at the described attitude α will result

$$C_L = \frac{4\pi^2 a_1 \sin\alpha}{1+\lambda} \tag{B6}$$

In addition, if the values of a_{2n+1} and $\sin\alpha_s$ are substituted into the following, an equation for the ordinates of the curve of total loading on the wing at α results.

$$c_l c_\eta = \frac{4SC_L}{\pi a_1 b} (a_1 \sin\varphi + a_3 \sin 3\varphi + a_5 \sin 5\varphi + a_7 \sin 7\varphi) \tag{B7}$$

If the values of coefficients obtained for a solution for the additional loading are then substituted into this expression, the additional loading at this coefficient will result. Subtraction of the ordinates of this last from those of the total loading curve will give those of the desired basic loading curve.

Correction for c_{l_α}

As in the method of Falkner, the error introduced into the solution by the assumption that all section lift-curve slopes c_{l_α} were 2π can be readily eliminated. If the actual c_{l_α} does not vary across the wing, the coefficients a_{2n+1} should be multiplied by the ratio of actual c_{l_α} to 2π. If the actual value does vary along the span, this ratio should be included in equation (3) as a function of the spanwise variable φ.

Computing Instructions

These instructions apply only to unyawed wings devoid of camber and/or twist.

If the local angle of attack $\sin\alpha$ is introduced into expression (B1) in place of the downwash ratio w/V, this expression can be written

$$1 = \sum_{n=0}^{3} (2n+1)a_{2n+1}(F_1+F_2+F_3F_3'-F_4F_4'+F_5F_5'+F_6F_6'+F_7F_7'+F_8F_8') \quad \text{(B8)}$$

where

$$F_1 = \frac{(-1)^n}{2n+1}\left(\frac{A_R}{B_R\sqrt{A^2_R+B^2_R}} - \frac{A_L}{B_L\sqrt{A^2_L+B^2_L}}\right)$$

$$F_2 = \frac{\pi}{s'\cos\Lambda}\,\frac{\sin(2n+1)\psi}{\sin\psi} \quad \text{(B9)}$$

$$F_3 = \frac{s'}{B^2_R}$$

Computing form B(1) is used to calculate all factors which remain constant throughout the summations for any one control point: A_R, B_R, A_L, B_L, s', C, F_3, F_4, F_5, F_6, F_7, F_8. The computation form for those factors, which vary with n only throughout the summations for any one control point, is presented in form B(2). Computing form B(3) is used to apply Simpson's rule to the integration of F_3', F_4', F_5', F_6', F_7' and F_8'. The factor K_{2n+1}, which is independent of wing shape and so can be applied to all wings, was calculated from the relation

$$K_{2n+1} = \int_0^{2\pi} \frac{\cos(2n+1)\,d\varphi}{\cos\varphi - \cos\psi} \tag{B10}$$

and is presented in the following table:

Control point	n	K_{2n+1}
1	0	2.54928
	1	8.26392
	2	8.87752
	3	6.10976
2	0	2.47976
	1	4.58640
	2	-1.90944
	3	-4.63656
3	0	2.33120
	1	0.47920
	2	-3.47696
	3	3.39776
4	0	2.00112
	1	-1.92340
	2	1.38068
	3	-0.53112

The results of the integration are presented in form B(3). Form B(4) is the form in which the components F are multiplied together and the results are summed producing four equations, one for each control point. Lastly, the form for the simultaneous solution of these equations (reference 9) and the resulting values of the unknowns are presented in form B(5).

$\Lambda = -45^\circ 12'$ $\tan\Lambda = -1.0070$ $\sin\Lambda = -.70957$ $\cos\Lambda = .70463$ $\sin 2\Lambda = -.99998$ $\cos 2\Lambda = -.00698$

$\lambda = .376$ $(1-\lambda) = .624$ $AR = 2.99$ $s' = \frac{AR(1+\lambda)}{4\cos\Lambda} = 1.46039$

1	2	3	4	5	6	7	8	9	10	11	12	13	14	15	16	17	18
Control Point	ψ	$\eta = \cos\psi$	(3)×s'	(3)×(1-λ)	$\frac{1-(5)}{2}$	(6)sinΛ δ'	$\frac{(7)}{s'}$ δ'/s'	(3)+(7) A_R	(6)×cosΛ B_R	(4) ×sin2Λ	(10)+(11) B_L	(4) ×cos2Λ	(13)-(7) A_L	$(10)^2$	$(7)^2$	(15)+(16)	$-\sqrt{(17)}$
1	20°	.940	1.37277	.58656	.20672	-.14668	-.10044	1.22609	.14566	1.37274	1.23705	-.00968	1.3740	.03122	.02152	.04274	.20674
2	40°	.766															
3	60°	.500															
4	80°	.174															

19	20	21	22	23	24	25	26	27	28	29	30	31	32	33	34	35	36
$\frac{(18)}{(10)}$ C	$\frac{s'}{(12)^2}$ F_3	$\frac{(9)}{(10)}$	(21) +tanΛ	$\frac{(22)}{(10)}$ F_4	$\left[\frac{s'}{(10)}\right]^2$ f_5	(3)×s'	(9) -(25)	1+ $\frac{(26)\tan\Lambda}{(10)}$	(19)×s'	$\frac{(27)}{(28)}$ F_5	$\frac{s'}{(12)^2}$ F_6	$\frac{(14)}{(12)}$	(31) -tanΛ	$\frac{(32)}{(12)}$ F_7	(14) -(25)	1- $\frac{(34)\tan\Lambda}{(12)}$	$\frac{(35)}{s'}$ F_8
1.41933	48.33146	8.41748	7.41048	50.87572	100.52106	1.37277	-.14668	2.01406	2.07287	.97176	.96989	-.11173	.89527	-.72960	-.23567	2.01406	1.37277

(1.)

1	2	3	4	5	6	7	8	9	10	11	12	13	14
Control Point	n	$(9)^2_{B1}$	(3) $+(15)_{B1}$	$\sqrt{(4)}$	$\frac{(21)_{B1}}{(5)}$	$\frac{(31)_{B1}}{(5)}$	(6) -(7)	2(2) + 1	$\frac{(-1)^n}{(9)}$	(10)×(8)	(9)×$(2)_{B1}$	$\frac{\sin(12)}{\sin(2)_{B1}}$	$\frac{(13)\pi}{s\cos\Lambda}$
1	0	1.50330	1.52452	1.23477	6.31737	-.09049	6.90786	1	1.000000	6.90786	20	1	1.05297
	1												
	2												
	3												
2	0												
	1												

(2.)

NATIONAL ADVISORY COMMITTEE FOR AERONAUTICS

FORM B:— COMPUTING FORM FOR MUTTERPERL'S METHOD

(Underscored numbers are sample calculations)

Control Point – 1

A_R = 1.22609 B_R = .14566 A_L = .13710 B_L = – 1.22708 η = .940 δ'/s' = –.10044 C = 1.41933

1	2	3	4	5	6	7	8	9	10	11	12	13	14	15	16	17	18	19
n	ϕ	cos(2)	cos [(2)(1)+1] ×(3)	(3) $-\frac{A_R}{s'}$	(5) $\frac{s'}{B_R}$	$\sqrt{1+(6)^2}$	(3)×(9)	(4)/(7)	(3) $-\eta_1' + 2\frac{\delta}{s'}$	(7)+C	(9)×(10)/11	(4) $+\frac{A_L}{s'}$	(13) $\frac{s'}{B_L}$	$\sqrt{1+(14)^2}$	(3)×(17)	(4)/(15)	(3)+η	(17)/(18)
0	0	1.00000	1.00000	.16044	1.60857	1.89407	.52796	.52796	.26088	3.31340	.04157	1.09388	–.30186	1.64160	.60916	.60916	1.9400	.31400
	22.5																	
	45.0																	
	67.5																	
1	0																	
	15																	
	45																	
	60																	
	75																	
2	0																	
	9																	
	27																	
	36																	
	45																	
	63																	
	72																	
	81																	
3	0																	
	6.43																	
	19.29																	
	25.71																	
	32.14																	
	45.00																	
	51.43																	
	57.86																	
	70.71																	
	77.14																	
	83.57																	

(3)

FORM B:– CONTINUED

NATIONAL ADVISORY COMMITTEE FOR AERONAUTICS

1	2	3	4	5	6	7	8	9	10	11	12	13	14	15	16	17	18	19	20	21
Control Point	n	F_1	F_2	F_3'	F_4'	F_5'	F_6'	F_7'	F_8'	$F_3' \times F_3'$	$F_4' \times F_4'$	K_{2n+1}	$F_5' \times f_5$	(13)-(14)	$F_5' \times (15)$	$F_6' \times F_6'$	$F_7' \times F_7'$	$F_8' \times F_8'$	(3)+(4)+(11)+(12)+(16)+(17)+(18)+(19)	Coeff. of a_{2n+1} = (9)/(20) × (20)
1	0	4.90786	3.05296	46.83146	-50.89592	.97176	.96989	-.72960	1.37912	38.99446	-30.15012	2.54928	2.69396	-.18468	-.14059	.50989	-.52780	-.59847	15.04807	15.04507
	1																			
	2																			
	3																			
2	0																			
	1																			
	2																			
	3																			
3	0																			
	1																			
	2																			

(4)

Equation	1	2	3	4
constant	1	1	1	1
a_1	15.04507			
a_3	13.52088			
a_5	14.86189			
a_7	9.22302			

a_{2n+1}
+.094440
-.011127
+.006564
-.003545

(5)

FORM B:— CONCLUDED

NATIONAL ADVISORY COMMITTEE FOR AERONAUTICS

APPENDIX C.– DEVELOPMENT AND COMPUTING PROCEDURES FOR USE WITH THE WEISSINGER METHOD

In the German reports available, which described this method, the mathematical development was not complete. It was thought advisable therefore to include the development in the present paper.

From lifting-line theory the equation of downwash at the one-quarter chord line of a straight wing is given by

$$w_y = \frac{1}{4\pi}\int_{-b/2}^{b/2}\frac{\Gamma'(\overline{y})}{y-\overline{y}}\,d\overline{y} \tag{C1}$$

This integral equation is solved by Multhopp by an integration formula (reference 10).

The equation of downwash at any point xy of a straight wing is given by

$$w_{xy} = \frac{1}{4\pi}\int_{-b/2}^{b/2}\frac{1}{y-\overline{y}}\left[1 + \frac{\sqrt{x^2+(y-\overline{y})^2}}{x}\right]\Gamma'(\overline{y})\,d\overline{y} \tag{C2}$$

Weissenger divides this integral into two integrals, one of which is the same as equation (C1) which he solves by Multhopp's method; and the other which he solves by a method analagous to that of Multhopp.

The mathematical development is as follows:

With $G = \Gamma/bV$, $\eta = 2y/b$, $\overline{\eta} = 2\overline{y}/b$, $ar = b/c_\eta$

and setting x equal to the distance to the three-quarter chord line $x = c_\eta/2$, the equation (C2) becomes

$$\frac{w}{V} = \frac{1}{2\pi}\int_{-1}^{1}\frac{1}{\eta-\overline{\eta}}\left[1 + \sqrt{1+(ar)^2(\eta-\overline{\eta})^2}\right]G'(\overline{\eta})\,d\overline{\eta}$$

or

$$\frac{w}{V} = \frac{2}{2\pi}\int_{-1}^{1} \frac{G'(\overline{\eta})d\overline{\eta}}{\eta-\overline{\eta}} + \frac{ar}{2\pi}\int_{-1}^{1} L_{\Lambda}\left[ar(\eta-\overline{\eta})\right] G'(\overline{\eta})d\overline{\eta} \tag{C3}$$

where

$$L_{\Lambda=0}\left[ar(\eta-\overline{\eta})\right] = \frac{\sqrt{1+(ar)^2(\eta-\overline{\eta})^2}-1}{ar(\eta-\overline{\eta})} \tag{C4}$$

or

$$L_{\Lambda=0}(\nu,\mu) = L\left[ar(\cos\varphi_\nu - \cos\varphi_\mu)\right] = \frac{\sqrt{1+ar_\nu^2(\cos\varphi_\nu - \cos\varphi_\mu)^2}-1}{ar_\nu(\cos\varphi_\nu - \cos\varphi_\mu)}$$

The first integral of equation (C3) can be written as a function of φ.

$$\frac{1}{2\pi}\int_{-1}^{1} \frac{G(\overline{\eta})}{\eta-\overline{\eta}}\,d\overline{\eta} = \frac{1}{2\pi}\int_{0}^{\pi} \frac{\frac{dG(\varphi)}{d\varphi}\,d\varphi}{\cos\varphi - \cos\varphi_\nu} \tag{C5}$$

where

$$\cos\varphi_\nu = \cos\frac{\nu\pi}{m+1} = \frac{2y}{b} = \eta$$

An integration formula gives

$$\int_{-1}^{1} f(\overline{\eta})d\overline{\eta} = \frac{\pi}{m+1}\sum_{n=1}^{m} f(\overline{\eta}_n)\sin\varphi_n \tag{C6}$$

where $\varphi_n = \frac{n\pi}{m+1}$, $f(\overline{\eta}_n)$ is the value of $f(\overline{\eta})$ at $\overline{\eta}_n$.

Equation (C6) holds exactly if $f(\bar{\eta})$ can be represented by

$$f(\bar{\eta}) = \sqrt{1-\bar{\eta}^2} \sum_{\nu=0}^{2m-1} A_\nu \bar{\eta}^\nu = \sum_{\nu=1}^{2m} a_\nu \sin \nu\varphi$$

or, in addition,

$$f(\varphi) = \frac{2}{m+1} \sum_{n=1}^{m} f(\bar{\eta}_n) \sum_{\mu_1=1}^{m} \sin \mu_1\varphi_n \sin \mu_1\varphi \tag{C7}$$

Letting $G(\varphi) = f(\varphi)$

then

$$G(\varphi) = \frac{2}{m+1} \sum_{n=1}^{m} G_n \sum_{\mu_1=1}^{m} \sin \mu_1\varphi_n \sin \mu_1\varphi$$

$$\frac{dG}{d\varphi} = \frac{2}{m+1} \sum_{n=1}^{m} G_n \sum_{\mu_1=1}^{m} \mu_1 \sin \mu_1\varphi_n \times \cos \mu_1\varphi$$

and the integral in equation (C5) becomes

$$\frac{2}{m+1} \sum_{n=1}^{m} G_n \int_0^\pi \sum_{\mu_1=1}^{m} \mu_1 \frac{\sin \mu_1\varphi_n \cos \mu_1\varphi}{\cos \varphi - \cos \varphi_\nu} d\varphi$$

Now

$$\int_0^\pi \frac{\cos n\varphi}{\cos \varphi - \cos \varphi_o} d\varphi = \frac{\pi \sin n\varphi_o}{\sin \varphi_o} \tag{C8}$$

or

$$\int_0^\pi \sum_{\mu_1=1}^{m} (\mu_1 \sin \mu_1\varphi_\eta) \left(\frac{\cos \mu_1\varphi}{\cos \varphi - \cos \varphi_\nu}\right) d\varphi = \pi \sum_{\mu_1=1}^{m} \frac{\mu_1 \sin \mu_1\varphi_\eta \sin \mu_1\varphi_\nu}{\sin \varphi_\nu}$$

so that equation (C5) becomes

$$\left(\frac{1}{2\pi}\right)\left(\frac{2\pi}{m+1}\right)\sum_{m=1}^{m} G_n \sum_{\mu_1=1}^{m} \frac{\mu_1 \sin \mu_1\varphi_n \sin \mu_1\varphi_\nu}{\sin \varphi_\nu}$$

$$= \frac{1}{m+1} \sum_{n=1}^{m}{}' G_n \sum_{\mu_1=1}^{m} \frac{\mu_1 \sin \mu_1\varphi_n \sin \mu_1\varphi_\nu}{\sin \varphi_\nu} \tag{C9}$$

The μ_1 series is independent of wing geometry and may be put into a coefficient usable for all wings.

From equation (C9), for $n=\nu$, let

$$b_{\nu,\nu} = \frac{1}{(m+1) \sin \varphi_\nu} \sum_{\mu_1=1}^{m} \mu_1 \sin^2 \mu_1\varphi_\nu \tag{C10}$$

and for $n \neq \nu$, let

$$b_{\nu,n} = \frac{-1}{(m+1) \sin \varphi_\nu} \sum_{\mu_1=1}^{m} \mu_1 \sin \mu_1\varphi_n \sin \mu_1\varphi_\nu \tag{C11}$$

Then equation (C5) becomes

$$b_{\nu,\nu}G_\nu - \sum_{n=1}^{m}{}' b_{\nu,n} G_n \tag{C12}$$

(Note: The summation prime indicates that the term of $n = \nu$ should not be included.)

Expression (C12) gives the induced angle of attack on the one-quater-chord line, at the span station ν, in terms of the summation of n spanwise values of the dimensionless circulation.

Equations (C10) and (C11) may be simplified with the aid of the summation formula

$$\sum_{\mu_1=1}^{m} \mu_1 \cos \mu_1 x = \text{real part of}\left(\sum_{\mu_1=1}^{m} \mu_1 e^{i\mu_1 x}\right)$$

$$= \frac{m \cos(m+1)x - (m+1)\cos mx + 1}{2(\cos x - 1)}$$

or

$$b_{\nu,\nu} = \frac{m+1}{4 \sin \varphi_\nu} \tag{C13}$$

$$b_{\nu,n} = \frac{\sin \varphi_n}{(\cos \varphi_n - \cos \varphi_\nu)^2}\left[\frac{1-(-1)^{n-\nu}}{2(m+1)}\right] \tag{C14}$$

The second integral of the integral equation (C3) or

$$\frac{1}{2\pi}\int_{-1}^{1} I_A(\nu,\mu)G'(\overline{\eta})d\overline{\eta} \tag{C15}$$

is solved in an analogous fashion.

The integration formula gives

$$\int_0^\pi f(\varphi)d\varphi = \frac{\pi}{M+1}\left[\frac{f(\varphi_0)+f(\varphi_{M+1})}{2} + \sum_{\mu=1}^{M} f(\varphi_\mu)\right] \tag{C16}$$

where

$$\varphi_\mu = \frac{\mu\pi}{M+1}$$

Dimensionless circulation is given by

$$G(\varphi) = \frac{2}{m+1} \sum_{n=1}^{m} G_n \sum_{\mu_1=1}^{m} \sin \mu_1\varphi_n \sin \mu_1\varphi$$

or

$$G'(\varphi) = \frac{2}{m+1} \sum_{n=1}^{m} G_n \sum_{\mu_1=1}^{m} \mu_1 \sin \mu_1 \varphi_n \cos \mu_1\varphi$$

Letting

$$f_n(\varphi) = \frac{2}{m+1} \sum_{\mu_1=1}^{m} \mu_1 \sin \mu_1\varphi_n \cos \mu_1\varphi \tag{C17}$$

then

$$G'(\varphi) = \sum_{n=1}^{m} G_n f_n(\varphi)$$

Expression (C15) may be modified so that

$$\frac{1}{2\pi}\int_{-1}^{1} L_\Lambda(\nu,\mu)\ G'(\overline{\eta})d\overline{\eta} = -\frac{1}{2\pi}\int_{0}^{\pi} L_\Lambda(\nu,\mu)G'(\varphi)d\varphi$$

$$= \sum_{n=1}^{m} -\frac{1}{2\pi}\int_{0}^{\pi} \left[L_\Lambda(\nu,\mu)G_n\ f_n(\varphi)\right] d\varphi$$

Then applying equation (C16), $\frac{1}{2\pi}\int_{-1}^{1} L_\Lambda(\nu,\mu)\ G'(\overline{\eta})d\overline{\eta}$

$$= -\frac{1}{2\pi}\sum_{n=1}^{m}\frac{\pi}{M+1} G_n\left\{\frac{[L_\Lambda(\nu,o)](f_{n,o})[L_\Lambda(\nu,M+1)](f_{n,M+1})}{2} + \sum_{\mu=1}^{M} L_\Lambda(\nu,\mu)f_{n,\mu}\right\}$$

$$= \sum_{n=1}^{m} G_n \frac{-1}{2(M+1)}\left\{\frac{[L_\Lambda(\nu,o)](f_{n,o})+[L_\Lambda(\nu,M+1)](f_{n,M+1})}{2} + \sum_{\mu=1}^{M} L_\Lambda(\nu,\mu)f_{n,\mu}\right\}$$

For simplicity let $f_{n,\mu} = f_n(\varphi_\mu)$ where $f_n(\varphi_\mu)$ is from equation (C17) for $\varphi = \varphi_\mu = \mu\pi/M+1$

Then if

$$g_{\nu,n} = -\frac{1}{2(M+1)}\left\{\frac{[L_\Lambda(\nu,o)](f_{n,o})+[L_\Lambda(\nu,M+1)](f_{n,M+1})}{2} + \sum_{\mu=1}^{M} L_\Lambda(\nu,\mu)f_{n,\mu}\right\} \tag{C18}$$

expression (C15) becomes

$$\sum_{n=1}^{m} G_n g_{\nu,n} \tag{C19}$$

The solution of equation (C3) is two times equation (C12) plus ar_ν times equation (C19) or

$$\frac{W}{V} = 2\left(b_{\nu,\nu}G_\nu - \sum_{n=1}^{m}{}' b_{\nu,n}\, G_n\right) + \sum_{n=1}^{m} ar_\nu\, g_{\nu,n}\, G_n$$

$$= 2\, b_{\nu,\nu}\, G_\nu + ar_\nu\, g_{\nu,\nu}\, G_\nu + \sum_{n=1}^{m}{}' ar_\nu\, g_{\nu,n}\, G_n - 2\sum_{n=1}^{m}{}' b_{\nu,n}G_n$$

so that

$$\frac{W}{V} = (2b_{\nu,\nu} + ar_\nu\, g_{\nu,\nu})\, G_\nu - \sum_{n=1}^{m}{}' (2b_{\nu,n} - ar_\nu\, g_{\nu,n})\, G_n$$

or

$$\frac{W}{V} = b^*_\nu\, G_\nu - \sum_{n=1}^{m}{}' b^*_{\nu,n}\, G_n \tag{C20}$$

where

$$b^*_\nu = 2b_{\nu,\nu} + ar_\nu g_{\nu,\nu}$$
$$b^*_{\nu,n} = 2b_{\nu,n} - ar_\nu \quad g_{\nu,n} \tag{C21}$$

The prime on the summation indicates that the term of $n = \nu$ should not be added into it.

Equating the downwash to the local angle of attack of the plate,

$$\alpha_\nu = b^*_\nu G_\nu - \sum_{n=1}^{m}{}' b^*_{\nu,n} G_n \tag{C22}$$

For a swept wing the equation of downwash at any chordwise point for $y \geq 0$ is given by

$$\begin{aligned} w_{xy} = {} & \frac{1}{4\pi}\int_{-b/2}^{b/2} \frac{\Gamma'(y)}{y-\bar{y}} \left[1 + \frac{x - |\bar{y}| \tan \Lambda}{\sqrt{(x - |\bar{y}| \tan \Lambda)^2 + (y-\bar{y})^2}} \right] dy \\ & + \frac{1}{4\pi}\int_{-b/2}^{0} \Gamma(\bar{y}) \frac{x - y \tan \Lambda}{[(x - |\bar{y}| \tan \Lambda)^2 + (y-\bar{y})^2]^{3/2}} d\bar{y} \\ & + \frac{1}{4\pi}\int_{0}^{b/2} \Gamma(\bar{y}) \frac{x - y \tan \Lambda}{[(x - |y| \tan \Lambda)^2 + (y-\bar{y})^2]^{3/2}} d\bar{y} \end{aligned} \tag{C23}$$

The first integral is the downwash due to the trailing vortex sheet and the last two integrals represent the velocity induced by the lifting line. By integrating the last two integrals by parts and rearranging into dimensionless quantities, the preceding integrals may be put in a form similar to equation (C3).

$$\alpha = \frac{2}{2\pi}\int_{-1}^{1} \frac{G'(\bar{\eta})}{\eta-\bar{\eta}} d\bar{\eta} + \frac{ar}{2\pi}\int_{-1}^{1} L_\Lambda(\eta,\bar{\eta}) \; G'(\bar{\eta}) \; d\,\bar{\eta} \tag{C24}$$

(Note that in the following equation (C25) the squares under the second radical of $L_\Lambda(\eta,\bar{\eta})$ for $\bar{\eta} \leq 0$ are summed. In reference 3 these were erroneously shown as a difference.)

where for $\bar{\eta} \leq 0$

$$L_\Lambda(\eta,\bar{\eta}) = \frac{1}{ar(\eta-\bar{\eta})}\left\{\frac{\sqrt{[1+ar\tan\Lambda\,(\eta-|\bar{\eta}|)]^2+(ar)^2(\eta-\bar{\eta})^2}}{1+2\eta\,(ar)\tan\Lambda}-1\right\}+\frac{2\tan\Lambda\sqrt{[1+\eta(ar)\tan\Lambda]^2+(ar)^2\eta^2}}{1+2\eta\,(ar)\tan\Lambda}$$

and for $\bar{\eta} \geq 0$

$$L_\Lambda(\eta,\bar{\eta}) = \frac{\sqrt{[1+ar\tan\Lambda\,(\eta-|\bar{\eta}|)]^2+(ar)^2(\eta-\bar{\eta})^2}-1}{ar\,(\eta-\bar{\eta})} \qquad (C25)$$

Equation (C24) with $L_\Lambda(\eta,\bar{\eta})$ as given by equation (C25) is for $y \geq 0$ and will give values for only the positive span stations. For values with $y \leq 0$, expressions similar to equations (C23) and (C25) must be derived. Values of $L_\Lambda(\eta,\bar{\eta})$ are needed for $y \leq 0$ if an unsymmetrical wing is to analyzed.

Equation (C25) with $\eta = \cos\varphi_\nu$ and $\bar{\eta} = \cos\varphi_\mu$, and ar at span station ν as ar_ν for $\cos\varphi_\nu \geq 0$ becomes, for $\cos\varphi_\mu \leq 0$,

$$L_\Lambda(\nu,\mu) = \frac{1}{ar_\nu\,(\cos\varphi_\nu-\cos\varphi_\mu)}\left\{\frac{\sqrt{[1+ar_\nu\tan\Lambda\,(\cos\varphi_\nu-|\cos\varphi_\mu|)]^2+(ar_\nu)^2(\cos\varphi_\nu-\cos\varphi_\mu)^2}}{1-2\,ar_\nu\cos\varphi_\nu\tan\Lambda}-1\right\}$$

$$+\frac{2\tan\sqrt{[1+ar_\nu\tan\Lambda\cos\varphi_\nu]^2+(ar_\nu)^2\cos^2\varphi_\nu}}{1+2\,(ar_\nu)\cos\varphi_\nu\tan\Lambda}$$

and for $\cos\varphi_\mu \geq 0$

$$L_\Lambda(\nu,\mu) = \frac{\sqrt{[1+ar_\nu\tan\Lambda\,(\cos\varphi_\nu-|\cos\varphi_\mu|)]^2+(ar_\nu)^2(\cos\varphi_\nu-\cos\varphi_\mu)^2}-1}{ar_\nu\,(\cos\varphi_\nu-\cos\varphi_\mu)} \qquad (C26)$$

Equations for determining G_ν at spanwise points of $\frac{2y}{b} = \cos \frac{\nu\pi}{m+1}$ for any wing may therefore be determined from equation (C20).

Summarizing the computations, the relation equating downwash to the local slope of the plate at m points along the span giving m equations with m unknowns, G_η is

$$\alpha_\nu = b^*_\nu \; G_\nu - \sum_{n=1}^{m}{}' b^*_{\nu,n} \; G_n, \; \nu = 1,2, \ldots m$$

where

α_ν = angle of attack at span station ν

$$\frac{y}{b/2} = \cos \frac{\nu\pi}{m+1}$$

$$b^*_\nu = 2b_{\nu,\nu} + ar_\nu \; g_{\nu,\nu}$$

$$b^*_{\nu,n} = 2b_{\nu,n} - ar_\nu \; g_{\nu,n}$$

$$b_{\nu,\nu} = \frac{m+1}{4 \sin \varphi_\nu}$$

$$b_{\nu,n} = \frac{\sin \varphi_n}{(\cos \varphi_n - \cos \varphi_\nu)^2}\left[\frac{1-(-1)^{n-\nu}}{2(m+1)}\right]$$

$$g_{\nu,\nu} = g_{\nu,n} \text{ for } n = \nu$$

$$g_{\nu,n} = -\frac{1}{2(M+1)}\left[\frac{L_\Lambda(\nu,o)(f_{n,o}) + L_\Lambda(\nu,M+1)}{2} + \sum_{\mu=1}^{M} L_\Lambda(\nu,\mu) \; f_{n,\mu}\right]$$

$$ar_\nu = \frac{b}{c_\nu} = \frac{\text{wing span}}{\text{chord at span station } \nu}$$

$L_\Lambda(\nu,\mu)$, for a straight wing, see equation (C4).

$L_\Lambda(\nu,\mu)$, for a swept wing, see equation (C26).

$$f_{n,\mu} = \frac{2}{m+1} \sum_{\mu_1=1}^{m} \mu_1 \sin \mu_1 \quad \varphi_n \cos \mu_1 \quad \varphi_\mu$$

where again

$$\varphi_n = \frac{n\pi}{m+1}$$

$$\varphi_\nu = \frac{\nu\pi}{m+1}$$

$$\varphi_\mu = \frac{\mu\pi}{M+1}$$

The computations required in the preceding group of equations may be simplified if such values as $b_{\nu,\nu}$ $b_{\nu,n}$ for various m's, and $f_{n,\mu}$ for various m's and M's are tabulated. Then a solution for any wing consists of a substitution of wing geometry into the $L_\Lambda(\nu,n)$ function, equation (C4) or equation (C26), and a combination of the tabulated coefficients to obtain m simultaneous equations with m unknowns G_n.

The computations for a symmetrically loaded wing may be still further reduced by an alteration to the preceding equations and coefficients. For a symmetrical wing with or without camber and twist, the distribution of local angle of attack is symmetrical about the center of the wing or

$$\frac{\alpha_\nu + \alpha_{m+1-\nu}}{2} = \alpha_\nu$$

then

$$\alpha_\nu = \alpha_{m+1-\nu}$$

$$G_\nu = G_{m+1-\nu}$$

and

ν goes from 1 to $\frac{m+1}{2}$

n goes from 1 to m

μ goes from 1 to M

The summation terms can be written such that n from 1 to m becomes $n + m+1-n$ from 1 to $\frac{m-1}{2}$, and μ from 1 to M becomes $\mu + M+1-\mu$ from 1 to $\frac{M-1}{2}$. (For the cases $n = \frac{m+1}{2}$ and $\mu = \frac{m+1}{2}$ the coefficients are expressed as their former values as will be seen directly.)

Now if equation (C20) is expressed as

$$\alpha_\nu = (b^*_{\nu,\mu} + b^*_{\nu,M+1-\mu})\, G_\nu - \sum_{n=1}^{\frac{m+1}{2}}{}' (b^*_{\nu,n} + b^*_{\nu,m+1-n})\, G_n$$

where

$$n \neq \frac{m+1}{2}$$

$$\mu \neq \frac{M+1}{2}$$

$$\nu = 1,2, \frac{m+1}{2}$$

Then

$$\alpha_\nu = B^*_\nu\, G_\nu - \sum_{n=1}^{\frac{m+1}{2}} B^*_{\nu,n}\, G_n \tag{C28}$$

where

$$\begin{aligned} B^*_\nu &= b^*_{\nu,\mu} + b^*_{\nu,M+1-\mu} \quad \nu = 1,2 \ldots \frac{m+1}{2},\ \mu \neq \frac{M+1}{2} \\ B^*_{\nu,n} &= b^*_{\nu,n} + b^*_{\nu,m+1-n} \quad \nu = 1,2 \ldots \frac{m+1}{2},\ n \neq \frac{m+1}{2} \end{aligned} \tag{C29}$$

These coefficients may also be expressed as

$$\begin{aligned} B^*_\nu &= 2b_{\nu,\nu} + a_{r\nu}\, \bar{g}_{\nu,\nu} \\ B^*_{\nu,n} &= 2B_{\nu,n} - a_{r\nu}\, \bar{g}_{\nu,n} \end{aligned} \tag{C30}$$

where $B_{\nu,n}$ is limited in that $B_{\nu,n} = b_{\nu,n} + b_{\nu,m+1-n}$ for $n \neq \frac{m+1}{2}$ $B_{\nu,n} = b_{\nu,n}$ for $n = \frac{m+1}{2}$

To find $\bar{g}_{\nu,n}$ consider the expression for $g_{\nu,n}$

$$g_{\nu,n} = -\frac{1}{2(M+1)} \frac{[L_\Lambda(\nu,0)](f_{n,0}) + [L_\Lambda(\nu,M+1)](f_{n,M+1})}{2} + \sum_{\mu=1}^{M} L_\Lambda(\nu,M+1)\, f_{n,\mu}$$

The summation term of $g_{\nu,n}$ can be written for $n \neq \frac{m+1}{2}$

$$\sum_{\mu=1}^{M} L_\Lambda(\nu,\mu) f_{n,\mu} = \sum_{\mu=1}^{\frac{M-1}{2}} [L_\Lambda(\nu,\mu) f_{n,\mu} + L_\Lambda(\nu,M+1-\mu) f_{n,M+1-\mu} + L_\Lambda(\nu,\mu) f_{m+1-n,\mu} + L_\Lambda(\nu,M+1-\mu) f_{m+1-n,M+1-\mu}]$$

$$+\left[L_\Lambda(\nu,\tfrac{M+1}{2}) f_{n,\frac{M+1}{2}} + L_\Lambda(\nu\tfrac{M+1}{2}) f_{m+1-n,\frac{M+1}{2}} \right]$$

for $n = \frac{m+1}{2}$

$$\sum_{\mu=1}^{M} L_\Lambda(\nu,\mu)\, f_{n,\mu} = \sum_{\mu=1}^{\frac{M-1}{2}} [L_\Lambda(\nu,\mu) f_{n,\mu} + L_\Lambda(\nu,M+1-\mu)\, f_{n,M+1-\mu}] + \left[L_\Lambda(\nu,\tfrac{M+1}{2})\, f_{n,\frac{M+1}{2}} \right] \qquad \text{(C31)}$$

where as before

$$f_{n,\mu} = \frac{2}{m+1} \sum_{\mu_1=1}^{m} \mu_1 \sin \mu_1 \frac{n\pi}{m+1} \cos \mu_1 \frac{\mu\pi}{M+1} \tag{C32}$$

examination of equation (C32) will indicate that for $n = \frac{m+1}{2}$

$$\left[L_\Lambda\left(\nu,\frac{M+1}{2}\right) f_{n,\frac{M+1}{2}} \right] = 0$$

for $n \neq \frac{m+1}{2}$

$$L_\Lambda\left(\nu,\frac{M+1}{2}\right) f_{n,\frac{M+1}{2}} + L_\Lambda\left(\nu,\frac{M+1}{2}\right) f_{m+1-n,\frac{M+1}{2}}$$

have values only for even μ_1, but for even μ_1, $f_{n,\mu} = - f_{m+1-n,\mu}$ so that these terms equal zero.

Then equation (C31) becomes, for $n \neq \frac{m+1}{2}$,

$$\sum_{\mu=1}^{M} L_\Lambda(\nu,\mu) f_{n,\mu} = \sum_{\mu=1}^{\frac{M-1}{2}} [(f_{n,\mu} + f_{m+1-n,\mu}) L_\Lambda(\nu,\mu)$$

$$+ (f_{n,M+1-\mu} + f_{m+1-n,M+1-\mu}) L_\Lambda(\nu,M+1-\mu)]$$

and for $n = \frac{m+1}{2}$,

$$\sum_{\mu=1}^{M} L_\Lambda(\nu,\mu) f_{n,\mu} = \sum_{\mu=1}^{\frac{M-1}{2}} [(f_{n,\mu}) L_\Lambda(\nu,\mu) + (f_{n,M+1-\mu}) L_\Lambda(\nu,M+1-\mu)] \tag{C33}$$

Further examination of equation (C32) will show that for only the odd μ_1

$$f_{n,\mu} = - f_{n,m+1-\mu}$$

However, the second summation in equation (C33) has $n = \frac{m+1}{2}$ in which instance the even μ_1 terms in equation (C32) vanish, thus the second summation becomes

$$\sum_{\mu=1}^{\frac{M-1}{2}} f_{\frac{m+1}{2},\mu} \left[L_\Lambda(\nu,\mu) - L_\Lambda(\nu,M+1-\mu)\right]$$

The first summation in equation (C33) has terms of $f_{n,\mu} = -f_{m+1-n,\mu}$ and $f_{n,M+1-\mu} = -f_{m+1-n,M+1-\mu}$ for even μ_1 or the coefficients of $L_\Lambda(\nu,\mu)$ and $L_\Lambda(\nu,M+1-\mu)$ vanish for even μ_1. In addition $f_{n,\mu}+f_{m+1-n,\mu} = -f_{n,M+1-\mu}+f_{m+1-n,M+1-\mu}$ for odd μ_1 or the summation is

$$\sum_{\mu=1}^{\frac{M-1}{2}} (f_{n,\mu}+f_{m+1-n,\mu}) \left[L_\Lambda(\nu,\mu) - L_\Lambda(\nu,M+1-\mu)\right]$$

where $f_{n,\mu}+f_{M+1-n,\mu}$ is obtained from (C32) for the odd terms of μ_1.

Lastly,

$$\frac{(f_{n,o})L_\Lambda(\nu,o)+(f_{n,M+1})L_\Lambda(\nu,M+1)}{2} = \frac{(f_{n,o}+f_{m+1-n,o})L_\Lambda(\nu,o)+(f_{n,M+1}+f_{m+1-n,M+1})L_\Lambda(\nu,M+1)}{2} \quad \text{for } n \neq \frac{m+1}{2}$$

$$= \frac{(f_{n,o}+f_{m+1-n,o})\left[L_\Lambda(\nu,o)-L_\Lambda(\nu,M+1)\right]}{2} \quad \text{for } n = \frac{m+1}{2}$$

where $f_{n,o}+f_{m+1-n,o}$ is taken for only odd μ_1. And, for even μ_1 $f_{n,o} = f_{m+1-n,o}$. So that a factor $\bar{f}_{n,\mu}$ may be expressed as

$$\bar{f}_{n,\mu} = f_{n,\mu} \text{ for } n = \frac{m+1}{2} \text{ and odd } \mu_1$$

$$\bar{f}_{n,\mu} = f_{n,\mu}+f_{m+1-n,\mu} \text{ for } n \neq \frac{m+1}{2} \text{ and odd } \mu_1$$

$$\bar{f}_{n,\mu} = \frac{f_{n,o}+f_{m+1-n,o}}{2} \text{ for } n \neq \frac{m+1}{2},\ \mu=0 \text{ and odd } \mu_1$$

$$\bar{f}_{n,\mu} = \frac{f_{n,o}}{2} \text{ for } n = \frac{m+1}{2},\ \mu=0 \text{ and odd } \mu_1$$

and

$$\bar{g}_{\nu,n} = \frac{-1}{2(M+1)} \sum_{\mu=0}^{\frac{M-1}{2}} \bar{f}_{n,\mu} \left[L_\Lambda(\nu,\mu) - L_\Lambda(\nu,M+1-\mu)\right] \tag{C34}$$

Examining equation (C32)

$$f_{n,\mu} \sim \sin \mu_1 \frac{n\pi}{m+1}$$

$$f_{m+1-n,\mu} \sim \sin \mu_1 \frac{(m+1-n)\pi}{m+1} = \sin\left(\mu_1\pi - \frac{\mu_1 n\pi}{m+1}\right) = \sin \mu_1\pi \cos \frac{\mu_1 n\pi}{m+1} - \sin \frac{\mu_1 n\pi}{m+1} \cos \mu_1\pi$$

or when μ_1 is odd,

$$f_{m+1-n,\mu} \sim \sin \frac{\mu_1 n\pi}{m+1}$$

Thus

$$f_{n,\mu} = f_{m+1-n,\mu}$$

Then, as before

$$\bar{g}_{\nu,n} = \frac{-1}{2(M+1)} \sum_{\mu=0}^{\frac{M-1}{2}} f_{n,\mu} \left[L_\Lambda(\nu,\mu) - L_\Lambda(\nu,M+1-\mu)\right]$$

where finally

$$\left.\begin{aligned}
\bar{f}_{n,\mu} &= f_{n,\mu} \text{ for } n = \frac{m+1}{2} \text{ and odd } \mu_1 \\
\bar{f}_{n,\mu} &= 2f_{n,\mu} \text{ for } n \neq \frac{m+1}{2} \text{ and odd } \mu_1 \\
\bar{f}_{n,\mu} &= f_{n,\mu} \text{ for } n \neq \frac{m+1}{2},\ \mu = 0, \text{ and odd } \mu_1 \\
\bar{f}_{n,\mu} &= \frac{f_{n,\mu}}{2} \text{ for } n = \frac{m+1}{2},\ \mu = 0, \text{ and odd } \mu_1
\end{aligned}\right\} \tag{C35}$$

and

$$f_{n,\mu} = \frac{2}{m+1} \sum_{\mu_1=1}^{m} \mu_1 \sin \mu_1 \frac{n\pi}{m+1} \cos \mu_1 \frac{\mu\pi}{M+1}$$

A further simplification to $\bar{g}_{\nu,n}$ can also be effected. From the binomial theorem:

$$\begin{aligned}
\sqrt{a^2 + b^2} &= a + \frac{1}{2}\frac{b^2}{a} - \frac{1}{8}\frac{b^4}{a^3} + \frac{1}{16}\frac{b^6}{a^5} - \frac{5}{128}\frac{b^8}{b^7} + \ldots \\
&= a\left[1 + \frac{1}{2}\left(\frac{b}{a}\right)^2 - \frac{1}{8}\left(\frac{b}{a}\right)^4 + \frac{1}{16}\left(\frac{b}{a}\right)^6 - \frac{5}{128}\left(\frac{b}{a}\right)^8 + \ldots\right]
\end{aligned}$$

for $a > b$ (C36)

and

$$\begin{aligned}
\sqrt{a^2 + b^2} &= b + \frac{1}{2}\frac{a^2}{b} - \frac{1}{8}\frac{a^4}{b^3} + \frac{1}{16}\frac{a^6}{b^5} \ldots \\
&= a\left[\frac{b}{a} + \frac{1}{2}\left(\frac{1}{b/a}\right) - \frac{1}{8}\left(\frac{1}{b/a}\right)^3 + \frac{1}{16}\left(\frac{1}{b/a}\right)^5 - \frac{5}{128}\left(\frac{1}{b/a}\right)^7 + \ldots\right]
\end{aligned}$$

for $a < b$ (C37)

Now letting

$$T(t) = \sqrt{\frac{a^2 - b^2}{a}}$$

then for $t = \frac{b}{a}$

$$T(t) = 1 + \frac{1}{2} t^2 - \frac{1}{8} t^4 + \frac{1}{16} t^6 - \frac{5}{128} t^8 \quad \text{for } t < 1$$

or

$$T(t) = t + \frac{1}{2}\left(\frac{1}{t}\right) - \frac{1}{8}\left(\frac{1}{t}\right)^3 + \frac{1}{16}\left(\frac{1}{t}\right)^5 - \frac{5}{128}\left(\frac{1}{t}\right)^7 \quad \text{for } t > 1 \tag{C38}$$

Equation (C34) may be written

$$\bar{g}_{\nu,\mu} = \frac{-1}{2(M+1)} \sum_{\mu=0}^{\frac{M-1}{2}} \bar{f}_{n,\mu}\, \Delta L_\Lambda(\nu,\mu) \tag{C39}$$

where

$$\Delta L_\Lambda(\nu,\mu) = L_\Lambda(\nu,\mu) - L_\Lambda(\nu,M+1-\mu) \tag{C40}$$

This can also be written

$$\Delta L_\Lambda(\nu,\mu) = L_\Lambda(\eta,\bar{\eta}) - L_\Lambda(\eta,-\bar{\eta}) \tag{C41}$$

so that from equation (C25)

$$\begin{aligned}\Delta L_\Lambda(\nu,\mu) = {} & \frac{\sqrt{[1+ar_\nu(\eta-\bar{\eta}) \tan\Lambda]^2+[ar_\nu(\eta-\bar{\eta})]^2}}{ar_\nu(\eta-\bar{\eta})} \\ & - \frac{1}{1+2ar_\nu\eta \tan\Lambda} \frac{\sqrt{[1+ar_\nu(\eta-\bar{\eta}) \tan\Lambda]^2+[ar_\nu(\eta+\bar{\eta})]^2}}{ar_\nu(\eta+\bar{\eta})} \\ & - \frac{2\tan\Lambda}{1+2ar_\nu\eta \tan\Lambda} \sqrt{[1+ar_\nu\eta \tan\Lambda]^2+[ar_\nu\eta]^2} \\ & - \frac{2\bar{\eta}}{ar_\nu(\eta^2-\bar{\eta}^2)}\end{aligned} \tag{C42}$$

Then

$$\Delta L_\Lambda(\nu,\mu) = T(t_1) - \frac{1}{1+2ar_\nu\eta\tan\Lambda}\left[T(t_2) + T(t_3)\tan\Lambda\right]$$
$$- T(t_3)\tan\Lambda - \frac{1}{ar_\nu}\left(\frac{2\bar{\eta}}{\eta^2-\bar{\eta}^2}\right) \qquad \text{(C43)}$$

where

$$t_1 = \left|\frac{1}{ar_\nu(\eta-\bar{\eta})} + \tan\Lambda\right|$$
$$t_2 = \left|\frac{1}{ar_\nu(\eta+\bar{\eta})} + \frac{\eta-\bar{\eta}}{\eta+\eta}\tan\Lambda\right|$$
$$t_3 = \frac{ar_\nu\,\eta}{1+ar_\nu\,\eta\tan\Lambda}$$

and $T(t_1)$ takes the sign of $(\eta-\bar{\eta})$

$T(t_3)$ takes the sign of t_3

Several of the functions of equation (C43) are independent of wing parameters and may be tabulated for various η and $\bar{\eta}$.

Let $\beta_\nu = \frac{1}{ar_\nu}$, $K_1 = \frac{1}{\eta-\bar{\eta}}$, $K_2 = \frac{1}{\eta+\bar{\eta}}$, $K_3 = \frac{1}{\eta}$,

$$K_4 = \frac{2\bar{\eta}}{\eta^2-\bar{\eta}^2}, \quad K_5 = \frac{\eta-\bar{\eta}}{\eta+\bar{\eta}}$$

where, as before,

$$\eta = \cos\frac{\nu\pi}{m+1}, \quad \bar{\eta} = \cos\frac{\mu\pi}{M+1}$$

Then

$$\Delta L_\Lambda(\nu,\mu) = T(t_1) - \frac{1}{\frac{1+2\tan\Lambda}{\beta_\nu K_3}}\left[T(t_2) + T(t_3)\tan\Lambda\right]$$

$$- T(t_3)\tan\Lambda - \beta_\nu K_4 \tag{C44}$$

where

$$t_1 = \left|\beta_\nu K_1 + \tan\Lambda\right|$$

$$t_2 = \left|\beta_\nu K_2 + K_5\tan\Lambda\right|$$

$$t_3 = \frac{1}{\beta_\nu K_3 + \tan\Lambda}$$

and

$T(t_1)$ takes the sign of K_1

$T(t_3)$ takes the sign of t_3

In summary, for the symmetrically loaded wing,

$$\alpha_\nu = B^*_\nu G_\nu - \sum_{m=1}^{\frac{m+1}{2}} B^*_{\nu,n} G_n, \quad \nu = 1,2 \ldots \frac{m+1}{2}$$

$$B^*_\nu = 2b_{\nu,\nu} + ar_\nu \bar{\varepsilon}_{\nu,\nu}$$

$$B^*_{\nu,n} = 2B_{\nu,n} - ar_\nu \bar{\varepsilon}_{\nu,n}$$

$$B_{\nu,n} = \begin{cases} b_{\nu,n} + b_{\nu,m+1-n} & \text{for } n \neq \frac{m+1}{2} \\ b_{\nu,n} & \text{for } n = \frac{m+1}{2} \end{cases}$$

$$b_{\nu,\nu} = \frac{m+1}{4\sin\varphi_\nu}$$

$$b_{\nu,n} = \left[\frac{\sin\varphi_n}{(\cos\varphi_n - \cos\varphi_\nu)^2}\right]\left[\frac{1-(-1)^{n-\nu}}{2m+1}\right]$$

$\bar{g}_{\nu,n}$ is taken from equation (C39); $\Delta L_\Lambda(\nu,\mu)$ is taken from (C44) and $\bar{f}_{n,\mu}$ is from equation (C35).

Limitation of the Series

The number of coefficients G_n required for accuracy depends upon how rapidly the series equation (3) converges. Weissinger used m equal to 7, 15, and 31 in his investigation and concluded that the results obtained with m equal to 7 were nearly as accurate as those with m equal to 15 or 31. For this reason m equal to 7, or four coefficients have been used in all of the applications of this method presented herein The number of terms required in the interpolation function $f_{n,\mu}$ must also be established. Again Weissinger used M equal to 7, 15, and 31 and found that results with M equal to 7 proved as satisfactory as those with M equal to 15 or 31. Lastly, it should be noted that equation (3) cannot satisfactorily approximate a curve containing discontinuities; however, a modification which will enable it to do so has been developed by Multhopp (reference 10).

Solution for Additional Loading

Since in a solution for additional loading the wing is considered a flat plate and all angles of attack α_ν are equal to α, equation (C28) may be modified to

$$1 = B^*_\nu \frac{G_\nu}{\alpha} - \sum_{n=1}^{\frac{m+1}{2}} B^*_{\nu,n} \frac{G_n}{\alpha} \tag{C45}$$

Evaluation of this equation at the several stations ν produces a set of equations containing the unknown circulations G_n which can then be solved simultaneously to obtain the values of these circulations.

Substitution of the values so obtained into the following expressions, results in the values indicated:

$$\frac{dC_L}{d\alpha} = \frac{\pi AR}{m+1} \sum_{n=1}^{m} \frac{G_n}{\alpha} \sin \varphi_n \tag{C46}$$

or for a symmetric wing,

$$\frac{dC_L}{d\alpha} = \frac{\pi AR}{m+1}\left(\frac{G_{\frac{m+1}{2}}}{\alpha} + 2\sum_{n=1}^{\frac{m-1}{2}} \frac{G_n}{\alpha} \sin \varphi_n\right) \tag{C47}$$

$$\frac{c_l}{C_L} = 2\ ar_v\ \frac{G_v}{\alpha}\ \frac{1}{dC_L/d\alpha} \tag{C48}$$

$$\frac{c_l c_v}{C_L c_{av}} = 2AR\ \frac{G_v}{\alpha}\ \frac{1}{dC_L/d\alpha} \tag{C49}$$

and from reference 11 for $m = 7$

$$\bar{\eta}_{cp} = \frac{0.3524G_1 + 0.503G_2 + 0.344G_3 + 0.0405G_4}{0.3827G_1 + 0.7071G_2 + 0.9239G_3 + 0.500G_4} \tag{C50}$$

Solution for Basic Loading

The basic loading on a wing with camber and/or twist can be determined in a manner exactly parallel to those of Falkner and Mutterperl. An arbitrary angle α_s is selected for the root section and the values α_{local}, measured from it. If these values are then substituted in equation (C28), and if the resulting equations are solved simultaneously, values of G_n will be obtained, which when inserted into the following expression will give the correct lift coefficient for the wing at this attitude.

$$C_L = \frac{\pi AR}{m+1}\left(\frac{G_{\frac{m+1}{2}}}{2} + 2\sum_{n=1}^{\frac{m-1}{2}} G_n \sin \varphi_n\right) \tag{C51}$$

If these values of G_n are also substituted into the following equation, an expression for the total loading curve will result.

$$c_l\ \ c_v = 2b\ G_v \tag{C52}$$

Of the values of G_n obtained from calculations for the additional loading are then substituted into equation (C52), ordinates of the additional loading curve will be obtained, which when subtracted from those of the total loading curve will give those of the desired basic loading curve.

Correction of c_{l_α}

As in the other methods, the error introduced by the assumption that the section lift-curve slope is in all instances 2π can be readily corrected. The correction is accomplished by modifying the specific circulation ordinates G_n by the ratio $\frac{\text{actual } c_{l_\alpha}}{2\pi}$ where specific values of this function at span station n must be determined if this function varies along the span.

Computing Instructions

The $\Delta L_\Lambda(\nu,\mu)$ functions are determined on form C(1) for a swept wing and form C(2) for a straight wing $(\Lambda_{0.25c} = 0)$. In both cases the coefficients K_1, K_2, K_3, K_4, and K_5 are obtained from table CI. In the values of $T(t_1)$, $T(t_2)$, $T(t_3)$ are obtained by entering chart CI with the values of t_1, t_2, t_3 from columns (10), (11), and (12) form C(1). Form C(3) contains those computations which result in the $\frac{m+1}{2}$ expressions containing the $\frac{m+1}{2}$ unknowns G_n. The values $\bar{g}_{\nu,n}$ in column 9 of form C(3) are obtained as follows: Consider the values in column 4 of this form as four groups of four members with the groups identified as

A when $n = 1$

B when $n = 2$

C when $n = 3$

D when $n = 4$

Similarly, the values in column 5 of this form can be considered grouped as

1 when $\nu = 1$

2 when $\nu = 2$

3 when $\nu = 3$

4 when $\nu = 4$

then

$$g_{1,1} = \Sigma A \times 1$$

$$g_{1,2} = \Sigma B \times 1$$

$$g_{1,3} = \Sigma C \times 1$$

$$g_{1,4} = \Sigma D \times 1$$

$$g_{2,1} = \Sigma A \times 2$$

$$g_{2,2} = \Sigma B \times 2, \text{ etc.}$$

The computing form for the simultaneous solution (reference 9) of the equation (C45) is given in form C(4). The equations are set up as follows: The first equation consists of the first four numbers in column 15 form C(3), the second equation the second four, and so forth; the first number in each group being the coefficient of G_1/α, the second being the coefficient of G_2/α and so forth. Simultaneous solution gives the G/α's with the corresponding span station.

$\Lambda = -45°12'$ $\tan\Lambda = -1.007$

$\lambda = .376$ $1-\lambda = .624$

$AR = 2.99$ $K = \frac{AR(1+\lambda)}{2} = 2.0571$

1	2	3	4	5	6	7	8*	9	10	11	12	13*	14	15	16*	17	18	19*	20
ν	μ	$1-\frac{(1-\lambda)}{K_3}$	$\beta_\nu = \frac{(3)}{K}$	$(4)K_1$	$(4)K_2$	$(4)K_3$	$(4)K_4$	$K_5 \times \tan\Lambda$	$t_1 = (5) + \tan\Lambda$	$t_2 = (6) + (9)$	$t_3 = \frac{1}{(7)+\tan\Lambda}$	$T(t_1)$	$T(t_2)$	$T(t_3)$	$(15) \times \tan\Lambda$	$\frac{1}{1+2\tan\Lambda}(7)$	$(14)+(16)$	$(17)\times(18)$	$\Delta L_{\nu\Lambda}(\nu,\mu) = (13^*) - (8^*) - (16^*) - (19^*)$
1	0	.4235	.2059	-.27056	.1070	.2229	-.28128	.0399	3.7126	.1469	1.8753	-.3846	.1011	.1613	.16243	-.1244	2.6353	-.3278	-2.330
	1																		
	2																		
	3																		
2	0																		
	1																		
	2																		
	3																		
3	0																		
	1																		
	2																		
	3																		
	0																		

COLUMN (13*) HAS SAME SIGN AS (5)
COLUMN (15) HAS SAME SIGN AS (12)
FOR $\mu = \nu$ COLUMN (13*) HAS THE VALUE (6) + tan Λ

(1.)

1	2	3	4	5	6	7*	8*	9*	10
ν	μ	$1-\frac{(1-\lambda)}{K_3}$	$\beta_\nu = \frac{(3)}{K}$	$t_1 = (4)K_1$	$t_2 = (4)K_2$	$(4)K_4$	$T(t_1)$	$T(t_2)$	$\Delta L_{\nu\Lambda}(\nu,\mu) = (8^*) - (7^*) - (9^*)$
1	0								
	1								
	2								
	3								
2	0								
	1								
	2								
	3								
3	0								
	1								
	2								

COLUMN (8*) HAS SAME SIGN AS (5)
FOR $\mu = \nu$ COLUMN (8*) HAS THE VALUE OF COLUMN (6)

(2.)

NATIONAL ADVISORY
COMMITTEE FOR AERONAUTICS

FORM C:- COMPUTING FORM FOR WEISSINGER'S METHOD

(Underscored numbers are sample calculations.)

1	2	3	4	5	6	7	8	9	10	11	12	13	14	15
ν	n	μ	$\bar{f}_{n\mu}$ TABLE CII	$\Delta L_{\lambda}(\nu\mu)$ $(20)_{c1}$ or $(10)_{c2}$		ν	n	$\bar{g}_{\nu,n}$	$\frac{1}{16\beta_\nu} = \frac{1}{16(4)_{c1 \text{ or } c2}}$	(9)x(10)	$2B_{\mu n}$ TABLE CIII	(12) −(11)	$2b_{\mu\nu}$ TABLE CIV	Coef. of $\frac{G_n}{\alpha}$ (14) −(13)
1	1	0	2.613	-2.330		1	1	-.3602	-.3036	.1094	0	-.1094	10.4524	10.5618
		1	-1.414				2				3.8284		0	
		2	-1.531				3				0		0	
		3	.414				4				.2928		0	
2	2	0	-1.414			2	1				2.0720		0	
		1	2.696				2				0		5.6568	
							3							
							4							

(3.)

EQUATION	1	2	3	4
CONSTANT	1	1	1	1
G_1/α	10.5618			
G_2/α	-2.8647			
G_3/α	.2720			
G_4/α	-.1362			

n or ν	$\frac{G_n}{\alpha}$ or $\frac{G_\nu}{\alpha}$	SPAN STATION $\cos\frac{n\pi}{8}$
1	.1890	.9239
2	.3683	.7071
3	.5494	.3827
4	.6676	0

(4.)

NATIONAL ADVISORY
COMMITTEE FOR AERONAUTICS

FORM C – CONCLUDED

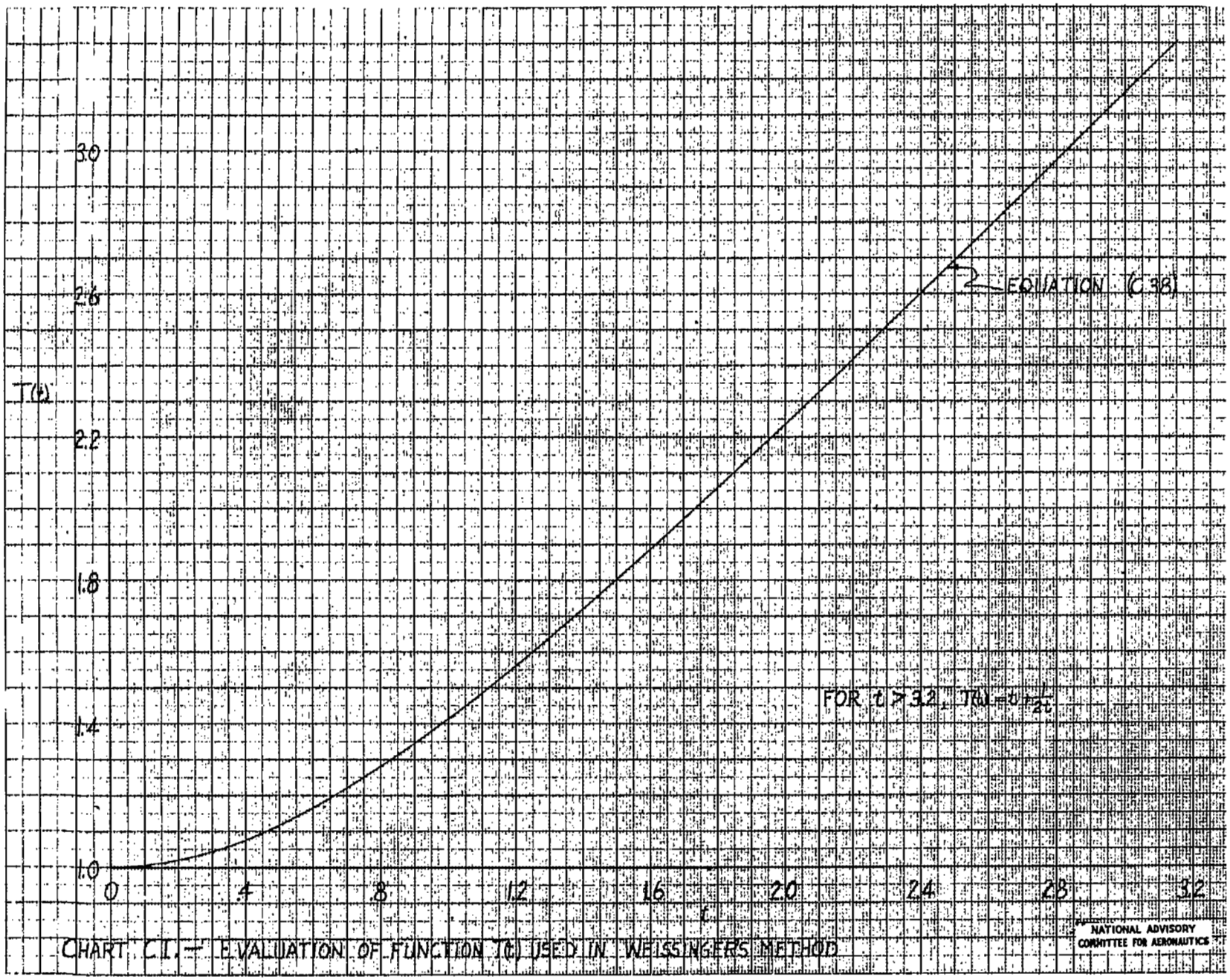

CHART C.I. — EVALUATION OF FUNCTION T(t) USED IN WEISSINGERS METHOD

TABLE CI.– CONSTANT FACTOR REQUIRED FOR THE CALCULATION OF $\Delta L_\Lambda(\nu,\mu)$ FOR m = M = 7

ν	μ	K_1	K_2	K_3	K_4	K_5
		$1/\eta-\bar{\eta}$	$1/\eta+\bar{\eta}$	$1/\eta$	$2\bar{\eta}/\eta^2-\bar{\eta}^2$	$\eta-\bar{\eta}/\eta+\bar{\eta}$
1	0	−13.1406	0.5198	1.0824	−13.6610	−0.0396
	1	∞	.5412	1.0824	∞	0
	2	4.6125	.6131	1.0824	3.9992	.1329
	3	1.8477	.7653	1.0824	1.0823	.4142
2	0	−3.4141	.5858	1.4142	−4.0000	−.1716
	1	−4.6125	.6131	1.4142	−5.2254	−.1329
	2	∞	.7071	1.4142	∞	0
	3	3.0826	.9176	1.4142	2.1650	.2977
3	0	−1.6200	.7232	2.6130	−2.3432	−.4464
	1	−1.8477	.7653	2.6130	−2.6128	−.4142
	2	−3.0826	.9176	2.6130	−4.0002	−.2977
	3	∞	1.3065	2.6130	∞	0
4	0	−1.0000	1.0000	∞	−2.0000	−1.0000
	1	−1.0824	1.0824	∞	−2.1649	−1.0000
	2	−1.4142	1.4142	∞	−2.8284	−1.0000
	3	−2.6130	2.6130	∞	−5.2260	−1.0000

TABLE CII.– INTERPOLATION FUNCTION $\bar{f}_{n,\mu}$ AS CALCULATED WITH m = M = 7

n	μ	$\bar{f}_{n,\mu}$
1	0	2.613
	1	-1.414
	2	-1.531
	3	.414
2	0	-1.414
	1	2.696
	2	-1.000
	3	-1.531
3	0	1.082
	1	-2.414
	2	3.696
	3	-1.414
4	0	- .500
	1	1.082
	2	-1.414
	3	2.613

TABLE CIII.– VALUES OF $B_{\nu,n}$ AS CALCULATED WITH m = 7

ν	n	$2B_{\nu,n}$
1	1	0
	2	3.8284
	3	0
	4	.2928
2	1	2.0720
	2	0
	3	2.3888
	4	0
3	1	0
	2	1.8284
	3	0
	4	1.7022
4	1	.2242
	2	0
	3	3.1548
	4	0

TABLE CIV.– VALUES OF $b_{\nu,\nu}$ AS CALCULATED WITH m = 7

ν	n	$2b_{\nu,\nu}$
1	1	10.4524
	2	----
	3	----
	4	----
2	1	----
	2	5.6568
	3	----
	4	----
3	1	----
	2	----
	3	4.3296
	4	----
4	1	----
	2	----
	3	----
	4	4.0000

REFERENCES

1. Falkner, V. M.: The Calculation of Aerodynamic Loading on Surfaces of Any Shape. R.&M. No. 1910, British A.R.C., 1943.

2. Mutterperl, William: The Calculation of Span Load Distributions on Swept-Back Wings. NACA TN No. 834, 1941.

3. Weissinger, J.: The Lift Distribution of Swept-Back Wings. NACA TM No. 1120, 1947.

4. McCormack, Gerald M., and Stevens, Victor I.: An Investigation of the Low-Speed Stability and Control Characteristics of Full-Scale Swept-Forward and Swept-Back Wings. NACA RM No. A6K15, 1946.

5. Falkner, V. M.: Calculations of the Aerodynamic Loading on a Sweptback Wing. Report No. 7322, British A.R.C., 1944.

6. Falkner, V. M.: Comparison of the Simple Calculated Characteristics of Four Sweptback Wings. Report No. 7446, British A.R.C., (British/U.S. Confidential), 1944.

7. Falkner, V. M.: Lifting Plane Theory of Wings with Discontinuities of Incidence. Rep. No. 8638, British A.R.C., (British/U.S. Restricted), 1945.

8. Falkner, V. M.: The Construction of Tables for Use in Calculating the Aerodynamic Loading of Wings. Rep. No. 7732, British A.R.C., (British/U.S. Restricted), 1944.

9. Margenau, Henry, and Murphy, George Moseley: The Mathematics of Physics and Chemistry. D. Van Nostrand Co., Inc., New York, 1943, pp. 480-483.

10. Multhopp, H.: Die Berechnung der Auftriebsverteilung von Tragflugeln. Luftf.-Forschg., Bd. 15 (1938).

11. Multhopp, H.: Die Anwendung der Tragflügeltheorie auf Fragen der Flugmechanik. Bericht S2 der Lilienthal - Ges. f. Luftf. - Forschg., Preisausschreiben, 1938-39.